Exact Solutions for Oldroyd-B Fluid over an Oscillating Plate

By

Khansa Mahmood

NATIONAL UNIVERSITY OF MODERN LANGUAGES

ISLAMABAD

21th April, 2025

Exact Solutions for Oldroyd-B Fluid over an Oscillating Plate

By

KHANSA MAHMOOD

MS Mathematics, National University of Modern Language, Islamabad, 2025

A THESIS SUBMITTED IN PARTIAL FULFILLMENT OF
THE REQUIREMENTS FOR THE DEGREE OF

MASTER OF SCIENCE

In **MATHEMATICS**

To

FACULTY OF ENGINEERING & COMPUTING

NATIONAL UNIVERSITY OF MODERN LANGUAGES ISLAMABAD

NATIONAL UNIVERSITY OF MODERN LANGUAGES FACULTY OF ENGINEERING & COMPUTER SCIENCE

THESIS AND DEFENSE APPROVAL FORM

The undersigned certify that they have read the following thesis, examined the defense, are satisfied with overall exam performance, and recommend the thesis to the Faculty of Engineering and Computing for acceptance.

Thesis Title: Exact Solutions for Oldroyd-B Fluid over an Oscillating Plate

Submitted By: Khansa Mahmood **Registration #:** 53/MS/MATH/S22

Master of Science in Mathematics (MS Math)
Title of the Degree

Mathematics
Name of Discipline

Dr. Asia Anjum _____
Name of Research Supervisor Signature of Research Supervisor

Dr. Sadia Riaz _____
Name of HoD (MATH) Signature of HoD

Dr. Muhammad Noman Malik _____
Name of Dean (FEC) Signature of Dean (FEC)

April 21th, 2025

AUTHOR'S DECLARATION

I Khansa Mahmood

Daughter of Pro. Mahmood-ul-Hassan

Registration # 53 /MS/MATH/S22

Discipline Mathematics

Candidate of **Master of Science in Mathematics (MS-MATH)** at the National University of Modern Languages do hereby declare that the thesis **Exact Solutions for Oldroyd-B Fluid over an Oscillating Plate** submitted by me in partial fulfillment of my MS degree is my original work and has not been submitted or published earlier. I also solemnly declare that it shall not, in future, be submitted by me for obtaining any other degree from this or any other university or institution. I also understand that if evidence of plagiarism is found in my thesis/dissertation at any stage, even after the award of a degree, the work may be canceled and the degree revoked.

Signature of Candidate

Khansa Mahmood
Name of Candidate

21th April 2025
Date

ABSTRACT

Title: Exact Solutions for Oldroyd-B Fluid over an Oscillating Plate

This thesis presents a comprehensive study of Oldroyd-B fluid over an oscillating plate. The primary focus is to analyze the steady-state, incompressible flow characteristics of an Oldroyd-B fluid. The solutions for the velocity field $u(y,t)$ and shear stress $\tau(y,t)$ are investigated. The governing equations are solved by integral transforms (Fourier sine and Laplace transforms). Both the results of the velocity field $u(y,t)$ and shear stress $\tau(y,t)$ are written in terms of convolutions theorem, elementary functions, and simple integral forms, satisfying all initial and boundary conditions. The obtained solutions are graphically analyzed for the variations of interesting flow parameters by using Mathematica software It has been observed that, when we increase relaxation time parameter the velocity profile also increases while shear stress decreases. On the other hand, when we increase retardation time parameter, the velocity profile along with shear stress decreases from maximum values to zero values. Moreover, the similar solutions for Maxwell, second-grade, and Newtonian fluid performing the same motions, are also obtained.

TABLE OF CONTENTS

Contents:

LIST OF FIGURES

LIST OF ABBREVIATIONS

BVP	Boundary value problem
IVP	Initial value problem
MATHEMATICA	Computation Program
ODEs	Ordinary differential equation
PDEs	Partial differential equation
UCM	Upper Convected Maxwell
GE	Governing Equation

LIST OF SYMBOLS

$u(y,t)$	-	Velocity field
$\tau(y,t)$	-	Shear stress
$u_s(y,t)$	-	Velocity field for sine oscillations
$\tau_s(y,t)$	-	Shear stress for sine oscillations
$u_c(y,t)$	-	Velocity field for cosine oscillations
$\tau_c(y,t)$	-	Shear stress for cosine oscillations
$u_N(y,t)$		Velocity field for Newtonian fluid
$H(t)$		Heaviside function
ν		Kinematic Viscosity
μ		Viscosity of the fluid
ξ		Fourier sine transform parameter
q		Laplace transform parameter
U		Non-zero constant
ω		Frequency
$\boldsymbol{A_1}$		First Rivlin-Erickson tensor
$\boldsymbol{S}$		Extra stress tensor
$\boldsymbol{T}$		Cauchy stress tensor
t		Time parameter
$\frac{d}{dt}$		Material derivative
$\frac{D}{Dt}$		Upper convective derivative
ρ		Density of the fluid
λ_1		Relaxation time parameter
λ_2		Retardation time parameter

ACKNOWLEDGMENT

There is no God but Allah and Muhammad (peace be upon him) is His messenger. I am solely obliged to Allah almighty for His blessings, my efforts were nothing, but His blessings enabled me to complete this project. My deepest gratitude to my mentor, my supervisor, Dr. Asia Anjum for her sincere guidance, time, and unreserved assistance in giving me relevant comments.

I express my kind gratitude to my sweet parents, my dear father, Prof. Mahmood ul Hassan, my lovely mother, Naeem Akhtar for their continuous support and care, and my sweet siblings for sure, this project is nothing but an outcome of their sincere support & prayers. I also proudly express my feelings of love for all my family members, who have always dreamed of a superior position for me.

I would also like to express my gratitude to the administration of the Department of Mathematics for their unwavering support during my research experience. Their assistance greatly simplified the challenges I encountered. Additionally, I extend my thanks to everyone who contributed significantly but was not specifically mentioned. Your help has been invaluable.

DEDICATION

I dedicate this project.

To ALLAH Almighty my creator, my strong pillar, my source of inspiration, wisdom, knowledge, and understanding.

To my beloved Father, whose trust and confidence in every phase of life has helped me to get along through thick and thin.

To my beloved Mother, what I and today is just because of her efforts.

CHAPTER 1

INTRODUCTION AND LITERATURE REVIEW

1.1 Oscillating plate

An oscillating plate is a rigid layer that moves periodically, either rotating or oscillating back and forth, within a fluid. This motion generates oscillatory fluid movement around the plate. Understanding the relationship between surrounding fluid flows and solid structures is often achieved by studying oscillating plates. The oscillation of a plate can be characterized by variables such as frequency, amplitude, and the type of motion (e.g., translational or rotational). Researchers frequently use experimental methods and mathematical simulations to investigate the fluid-structure interactions associated with oscillating plates. These innovations are increasingly being applied across various fields. Sheikholeslami *et al*. [1] investigated the effects of radiation and heat generation on the rapid magnetohydrodynamic (MHD) movement of a reflective and conductive nanofluid passing over an oscillating vertical plate in a porous medium. Patel *et al*. [2] examined the MHD flow of a Casson fluid over an oscillating perpendicular plate in a rotational system, considering the effects of accelerating wall temperature, wall radiation, heat generation, Hall currents, and chemical reactions. Ali Abro *et al*. [3] presented a mathematical analysis of an oscillating plate and extended it to fractional Burgers' fluid flow with electrical conduction. Reyaz *et al*. [4] investigated the effects of radiant heat on the MHD flow of a Casson fluid near an oscillating vertical plate, providing insights into fractional derivatives. Endalew *et al.* [5] studied how energy and mass transfer properties influence isotropic, inflexible Casson fluid flow over an oscillating plate. Farooq *et al.* [6] examined on the energy and mass transfer dynamics of oscillating Maxwell nanofluid flows. Asmat *et al.* [7] investigated Stokes' second problem, analyzing the motion of a semi-infinite, viscous, and insoluble fluid driven by an oscillating flat plate. Oscillating plates are used in various applications within fluid mechanics. It generates shear and turbulence, which enhances mixing in fluids, improving homogeneity in chemical processes or food production. Oscillating

plates can increase heat transfer rates by disturbing the boundary layer, which enhances convective heat transfer. Oscillating plates can be used to study the movement and deposition of particles in water channels or rivers. [8-9]

1.2 Maxwell Fluids

Maxwell fluids are fundamental for understanding and predicting the behavior of materials that do not fall strictly into the categories of purely elastic solids or purely viscous liquids. They provide a framework for analyzing complex, time-dependent responses. Zhang *et al.* [10] investigated the transformation of Maxwell fluids under slip and no-slip conditions into standard Maxwell fluids. They demonstrated that viscous fluids move more slowly than Maxwell fluids, while ordinary fluids move faster than fractional fluids. Hsiao *et al.* [11] examined an improved parameter control approach to an energy conversion problem in an industrial manufacturing system with temperature insertion. They examined energy transfer from mass to heat at a stagnation point, alongside the combined effects of electrical MHD Ohmic heating and forced and free convection airflow in an incompressible Maxwell fluid. Asif *et al.* [12] studied the flow induced by the movement of a flat bottom plate under slip boundary conditions, focusing on clasped flows of an incompressible Maxwell fluid with a non-integer order derivative and a non-unique kernel. Hayat *et al.* [13] examined a simplified model of the homogeneous-heterogeneous process for Maxwell fluid flow over a stretched surface. Riaz *et al.* [14] studied the time-dependent magnetohydrodynamic (MHD) flow of a Maxwell fluid with Newtonian heating effects near a vertical plate, employing a comparative approach. For fractional-time derivatives, the Caputo (C), Caputo-Fabrizio (CF), and Atangana-Baleanu (ABC) models were used to describe the Maxwell fluid's behavior. Yang *et al.* [15] examined the flow and heat transfer characteristics of a double fractional Maxwell fluid using a second-order slip model. Liu *et al.* [16] investigated rigid, steady, and homogeneous liquid edge flow and heat transfer along an oscillating plate. Abdeljawad *et al.* [17] analyzed the effects of heat generation and absorption on time-dependent MHD Maxwell fluid flow near an infinite plate immersed in a porous medium, considering startup velocity and increasing temperature. Megahed *et al.* [18] theoretically examined the MHD steady flow of a non-Newtonian Maxwell fluid driven by an elastic sheet placed within a porous medium under turbulent surface conditions. Asjad *et al.* [19] explored the unstable free convection flow of a

Maxwell fluid containing clay nanoparticles. Hanif *et al.* [20] investigated the two-dimensional boundary layer circulation and heat transfer of proportional Maxwell fluid with constant heating, presenting a novel Crank-Nicolson-based numerical algorithm.

1.3 Oldroyd-B Fluids

The Oldroyd-B fluid model is an essential framework in the study of viscoelastic fluids, providing tools to analyze and predict the flow behavior of materials with significant effects. It effectively captures the complex interplay between viscous and elastic properties. This concept was originally introduced by the British mathematician J.G. Oldroyd and is often used to describe the rheological properties of polymerized liquids or polymer solutions. Abbasi *et al.* [21] examined the Cattaneo-Christov heat transfer model for the flow of an incompressible Oldroyd-B fluid over a linearly stretched sheet in a two-dimensional stratified boundary layer. Their study included an analytical solution to boundary layer problems. Farooq *et al.* [22] investigated a computational framework to model the three-dimensional flow of Oldroyd-B fluids, incorporating the effects of Soret and Dufour numbers on combined convection. Elhanafy *et al.* [23] examined a normalized Galerkin least-squares finite element framework for digitally modeling Oldroyd-B viscoelastic fluids. Hafeez *et al.* [24] investigated the movement of Oldroyd-B fluids through a rotating disk, adopting the Cattaneo-Christov principles for mass and heat transfer. Shaqfeh *et al.* [25] studied detailed simulations and analyses of reduced polymer mixtures, emphasizing their behavior under Oldroyd-B flow dynamics. Khan *et al.* [26] studied the magnetohydrodynamic (MHD) flow of Oldroyd-B fluids over an oscillating disk, focusing on the regulation of heat and mass transfer. Awan *et al.* [27] examined the thermodynamic behavior of viscoelastic fluids, highlighting how delayed elasticity and stress onset can lead to relaxation and retardation phenomena. Their work specifically analyzed Oldroyd-B fluids under slip boundary conditions to better understand the distinctions between relaxation and retardation effects. Bashir *et al.* [28] investigated the behavior of a non-conducting, two-dimensional Oldroyd-B fluid flowing over a stretching sheet, including the formation of thermophoretic particles. Riaz *et al.* [29] examined the influence of external slip conditions on the flow of Oldroyd-B fluids over an infinitely stretching plate with consistent heating. Wang *et al.* [30] studied how an exponential basis

function approach modifies the hydrodynamic properties of fluids and its applicability in numerical simulations.

1.4 Integral Transform

Integral transforms are mathematical tools widely used in fluid mechanics to simplify complex equations and examine equations describing fluid dynamics. These transforms help express quantities in more manageable mathematical forms, enabling easier solutions to fluid flow problems. One of the most commonly used integral transforms in fluid mechanics is the Laplace transform. Additionally, other transforms, such as the Fourier transform, are also employed depending on the nature of the problem. Cotta *et al.* [31] examined the Generalized Integral Transform Technique (GITT), a hybrid numerical-analytical method designed to address flow problems involving mass and heat transfer. In another study, Cotta *et al.* [32] studied that fluid flow and transport in fractured porous media can be effectively resolved using GITT in conjunction with a single-domain reformulation approach and a coupled eigenvalue solution framework. Jafari *et al.* [33] investigated the importance of integral transforms in solving practical problems, showing that differential and integral equations can be reduced to simpler equations by selecting appropriate transforms. Mahfoud *et al.* [34] examined the effects of magnetic fields and buoyancy forces on vortex breakdown cycles in rotating electrically conducting fluids, utilizing GITT to analyze the phenomena. Cotta *et al.* [35] studied the application of GITT, illustrating that when combined with single-domain reformulation, it produces accurate, reliable, and cost-effective simulations for determining temperature distributions within a domain.

1.5 Exact Solutions

In fluid mechanics, the term "exact solutions" refers to analytical solutions of governing equations that describe the behavior of fluids. These solutions provide explicit computations for fluid motion under specific conditions, obtained through mathematical techniques such as integration, differentiation, and equation manipulation. Wang *et al.* [36] studied the oscillatory flow of a Maxwell fluid in an extended rectangular tube. They developed quantitative

computations for velocity profiles and phase distinctions, with a particular focus on analyzing the instabilities of the exact solutions. Jamil *et al.* [37] investigated the extended tackle approach to identify precise methods for characterizing complex and unstable magnetohydrodynamic (MHD) viscoelastic flow patterns within a porous medium. Murtaza *et al.* [38] studied the importance of exact solutions, noting that they serve as benchmarks for validating numerical and experimental results. Fetecau *et al.* [39] studied a detailed analysis to establish exact solutions for various unsteady flows of incompressible Upper-Convected Maxwell (UCM) fluids over a solid plate. Their study provided dimensionless formulations for velocity and stress fields. Baranovskii *et al.* [40] investigated the mechanical-to-thermal energy transfer in heat exchange equations. They derived new exact solutions for the longitudinal, non-isothermal flow of a second-grade fluid in a cylindrical duct with impermeable wall thicknesses. Their findings highlighted that atmospheric pressure imbalances, which are time-invariant, drive the fluid motion, while various boundary conditions were imposed on the stream walls.

1.6 Contributions to the Thesis

This thesis includes an overview of Abro *et al*. [42] has been introduced, followed by an expansion of the flow assessment by using Oldroyd-B fluid on an oscillating plate with Dirichlet boundary conditions. The main focus is to find an exact solution by using integral transforms (Fourier sine and Laplace transforms). The mathematical software Mathematica is utilized to construct graphs that explain the numerical outcomes. The impact of dimensionless elements is examined thoroughly.

1.7 Thesis Organization

An overview of the thesis's main points is given in the following:

Chapter 1 provides an introduction to the thesis and presents a summary of the main concepts and the research involved.

Chapter 2 provides some fundamental definitions, which are used during the research.

Chapter 3 provides a review work of Abro *et al*. [42].

Chapter 4 is the extended work of Abro *et al*. [42]. In this, we consider unsteady, incompressible Oldroyd-B fluid lies over an infinite flat plate. The solution of velocity field and shear stress are obtained from integral transforms.

Chapter 5 gives a summary of the entire research work and the potential future research applications.

References the Appendix includes a compilation of sources examined during the course of this thesis.

CHAPTER 2

BASIC DEFINITIONS

2.1 Fluid Mechanics

Examination of the movement of fluids, which is the study of how liquids behave when they are moving or at rest, as well as how fluids interact with solids or other fluids at boundaries, is known as fluid mechanics. [41]

2.2 Fluid

Anything that has no shape and can flow is called a fluid. It is a state of matter that can be identified by its capacity to change shape and adopt the form of its surroundings. Both gases and liquids are considered fluids. [41]

2.3 Flow

The movement or motion of a fluid is referred to as flow in fluid mechanics. Various forms of flow are defined as follows.

2.3.1 Steady/unsteady Flow

When there is steady flow, the fluid's velocity never changes over time; when there is unsteady flow, the velocity varies. Unsteady flow is exemplified by flow around an oscillating

airfoil or beginning flow within a channel, while laminar flow within a station at a constant rate is termed as steady flow.

2.3.2 Laminar / Turbulent Flow

Smooth, clearly defined streamlines and organized movement of fluids are features of laminar flow, such as raindrops, pollen, and blood cells in plasma. On the other hand, chaotic and irregular motion, frequently accompanied by swirling vortices, characterizes turbulent flow. Typical examples of turbulent flow are seen in blood circulation through arteries and the transportation of oil in pipelines, flow through pumps then turbines, and the wake created by boats.

2.3.3 Compressible / Incompressible Flow

When a fluid's density is greatly impacted by changes in temperature and pressure, compressible flow takes place, such as shaving cream, oxygen cylinders, pump, etc. Incompressible flow is a kind of fluid flow where the fluid's density either stays almost constant or barely changes while the fluid is moving such that minimal density changes occur in incompressible flows. Oil, honey, and water are examples of incompressible flow.

2.4 Stress

Fluid stress can be characterized as the force per unit area exerted an opposing direction to a small surface element within the fluid.

$$\text{Stress} = \frac{\text{Force}}{\text{Area}} . \tag{2.1}$$

It is measured in Nm^{-2} or in SI system and has dimensions $[\frac{M}{LT^2}]$.

2.4.1 Shear Stress

In fluid mechanics, the force imparted to a liquid per unit area is known as shear stress

which is parallel to a specific surface. It symbolizes a fluid's internal resistance to deformation in the presence of parallel forces. There is no shear stress in a fluid when it is at rest. [41]

2.5 Viscosity

A liquid has internal resistance to flow when it moves. This resistance to shear or flow is measured by viscosity. Simply, it indicates how "thick" or "sticky" a fluid is, or how easily it can flow. Two ways to characterize viscosity are as follows:

2.5.1 Dynamic Viscosity

Absolute viscosity (μ), sometimes known as dynamic viscosity, is a measurement of the proportion of shear stress to velocity gradient i.e.,

$$\mu = \frac{\text{Shear Stress}}{\text{Velocity gradient}} . \tag{2.2}$$

The dynamic viscosity is measured in $\frac{Ns}{m^2}$ or kg / m.s (SI. System) and the relevant dimensions are mentioned to be $[\frac{M}{LT}]$.

2.5.2 Kinematic Viscosity

The relationship among density and total viscosity be shown using kinematic viscosity. It can be expressed as,

$$\nu = \frac{\mu}{\rho} . \tag{2.3}$$

It has units of $\frac{m^2}{s}$ and the dimensions are $[\frac{L^2}{T}]$

2.6 Newtonian Fluid

A liquid is referred to as Newtonian when its viscosity doesn't change regardless of the shear stress applied to it. The viscosity law of Newton is followed, arguing that the shear rate of the fluid is exactly proportional to its shear stress. Mostly gases, water, and air are some examples of Newtonian fluids. [41]

2.7 Non-Newtonian Fluid

It states that in a fluid, the shear rate and the shear stress are directly correlated. The connection among shear stress and shear rate is more complicated in non-Newtonian fluids, and the viscosity can change depending on the applied stress or the rate of deformation. Some examples are blood, ketchup, and toothpaste. [41]

2.8 Viscoelastic Fluids

Materials that possess both flexible and sticky qualities are called viscoelastic fluids. In contrast to materials that are only viscous (like flows) or purely elastic (like solids), viscoelastic fluids exhibit both characteristics and respond to applied stress or deformation in a manner that varies over time. The primary categories of viscoelastic fluids are:

2.8.1 Maxwell Fluids

A Maxwell fluid is the simplest model viscoelastic material showing the properties of a typical liquid. On the long timescale, it shows viscous flow, but there is also extra elastic resistance to quick deformations.

2.8.2 Oldroyd-B Fluids

Viscoelastic behavior takes on a more sophisticated and universal form in the Oldroyd-B model. It has components that are both elastic and viscous, as well as a parameter that describes the material's retardation time. When describing the rheological structure of specific polymer compounds and polymer approaches, the Oldroyd-B model is widely used.

2.9 Rheological Behavior

In order to understand how materials flow and deform, rheology analyzes how their mechanical characteristics change in response to different forces, strains, and deformation rates.

2.10 Relaxation/ Retardation Time Parameter

Relaxation time can refer to the time it takes for a fluid to return in its equilibrium flow state after being disturbed. Relaxation time typically refers to the time it takes for stress to relax under a constant strain (a measure of how stress decreases over time), while retardation time focuses on the strain's time-dependent improvement under persistent stress. Although they characterize different features of the time-dependent response, both parameters are essential for understanding the viscoelastic behavior of materials.

2.11 Laplace Transform

Laplace transforms are used in the study of fluid dynamics to simplify the solution of linear ordinary and partial differential equations by converting them into algebraic equations. The Laplace transform $\mathcal{L}\{f(t)\}$ of a function $f(t)$ is demarcated as:

$$\mathcal{L}\{f(t)\} = F(s) = \int_0^\infty e^{-st}\ f(t)dt. \tag{2.4}$$

The inverse Laplace transform is defined as:

$$\mathcal{L}^{-1}\{F(s)\} = f(t) = \frac{1}{2\pi i}\int_0^{\infty} e^{st}F(s)\,ds. \tag{2.5}$$

2.12 Fourier Sine Transform

A function defined on the interval [0, ∞) can be transformed mathematically into an appropriate function in the domain of frequency via the Fourier Sine Transform. The Fourier sine transform $\mathcal{F}_s(\xi)$ of the function $f(x)$ is well-defined by means of:

$$\mathcal{F}_s\,(\xi) = \sqrt{\frac{2}{\pi}}\ \int_0^{\infty} sin(\xi x)\, f(x)dx, \tag{2.6}$$

to recover the original function $f(x)$ from its Fourier sine transform $\mathcal{F}_s\,(\xi)$, we use the inverse Fourier sine transform, which is given by:

$$f(x) = \mathcal{F}_s{}^{-1}\{\mathcal{F}_s\,(\xi)\} = \sqrt{\frac{2}{\pi}}\ \int_0^{\infty} \mathcal{F}_s\,(\xi) sin(\xi x)\,d\xi. \tag{2.7}$$

Choices of Integral Transforms:

1. **Fourier Transform**
   - **Use Case**: For analyzing functions with infinite or periodic domains.
   - **Domain**: $(-\infty,\infty)$
   - **Best for**: Frequency domain analysis.
2. **Laplace Transform**
   - **Use Case**: For functions defined on $[0,\infty)$.
   - **Domain**: $[0,\infty)$
   - **Best for**: Solving ODEs/PDEs with initial conditions.
3. **Fourier Sine and Cosine Transforms**
   - **Use Case**: For functions defined on $[0,\infty)$.
   - **Domain**: $[0,\infty)$.
   - **Best for**: Boundary value problems.

2.13 Heaviside Function

Step modifications to pressure, velocity, or other liquid-related quantities are frequently represented by the Heaviside function in fluid mechanics. In other words, at $t = 0$, the step function $u(t)$ "turns on", a changeover from 0 to 1. As a mathematical tool, it describes events like the abrupt start or stop of a fluid flow by expressing abrupt changes in conditions at a specific time.

2.14 Oscillatory Flows

When fluid properties, like density, pressure, or velocity, move in predictable and periodic ways around a central or equilibrium state, it's referred to as oscillation in fluid dynamics. Fluids can exhibit oscillatory flow patterns, particularly when there are recurring modifications to the boundary conditions or outside forces. Two instances are the oscillating motion in reciprocating pumps and the oscillatory flow in pipes.

2.15 Equation of Continuity

A key idea in fluid dynamics is the continuity equation, which explains how mass is conserved in fluid that moves. According to this, the rate of mass flow into any given fluid volume must equal the rate of mass flow out of that volume, plus any net mass buildup within the volume, for a fluid to be considered incompressible. In mathematics, the point of divergence of the motion of a fluid field is commonly employed to express the continuity equation. For an incompressible fluid in three dimensions, the continuity equation can be written as:

$$\boldsymbol{\nabla}.\boldsymbol{V} = 0, \tag{2.8}$$

where $\boldsymbol{V}$ is the viscosity of the fluid.

2.16 Momentum Equation

This equation shows implies the system's total momentum will constantly be conserved because it is physically tied to the law of conservation of momentum. When considering an incompressible fluid, the equation can be expressed as follows:

$$\rho \frac{d\boldsymbol{V}}{dt} = div\, \boldsymbol{\tau} + \rho \boldsymbol{b}\,, \tag{2.7}$$

where ρ relates to density, $\boldsymbol{V}$ is velocity, $\boldsymbol{\tau}$ defines the Cauchy stress tensor, $\rho \boldsymbol{b}$ refers to body force per unit area.

CHAPTER 3

Exact Solutions for Maxwell Fluid over an Oscillating Plane

3.1 Introduction

This chapter contains the precise solutions for Maxwell fluid over an oscillating plate are observed. The solutions for the Maxwell fluid's velocity field $u(y,t)$ and the shear stress $\tau(y,t)$ using integral transforms (Laplace and Fourier Sine transforms), solutions are found. All initial and boundary conditions are satisfied by the formulas for the shear stress $\tau(y,t)$ and the velocity field $u(y,t)$. The results are graphically displayed, and the influence of various parameters is discussed. Further, the result under the limiting conditions is found to be in good agreement with the existing one. This chapter provides a detailed review of the research paper [42].

3.2 Mathematical Formulation

Consider the area that lies over the surface of a plate that is perpendicular to y $-$axis is filled with an incompressible Maxwell fluid. The fluid is at rest when $t \leq 0$, and the surface of the plate is suddenly caused to a constant velocity U in its own plane at $t = 0^{+}$. The fluid is moved slowly and gradually above the plate as a result of the tangential shear stress. For the Maxwell liquid over a fluctuating plate, the outcomes are found by solving the differential equations that govern via the integral changes approach (Fourier sine and Laplace transform). The Cauchy's stress tensor in a Maxwell fluid is of the following form;

$$\boldsymbol{T} = -p\boldsymbol{I} + \boldsymbol{S}, \quad \boldsymbol{S} + \lambda_1 \frac{D\boldsymbol{S}}{Dt} = \mu \boldsymbol{A_1}\,, \tag{3.1}$$

in which $\boldsymbol{T}$ stands for the stress tensor of Cauchy, $-p\boldsymbol{I}$ symbolizes the unidentified spherical stress, the extra stress tensor is denoted by $\boldsymbol{S}$, relaxation time is represented by λ_1, the viscosity is denoted by μ, the first Rivlin-Ericksen tensor is $\boldsymbol{A_1}$ and $\frac{D}{Dt}$ stands upper convective derivative is defined as.

$$\frac{D\boldsymbol{S}}{Dt} = \frac{d\boldsymbol{S}}{dt} - \boldsymbol{LS} - \boldsymbol{SL^T}, \tag{3.2}$$

where

$$\boldsymbol{L} = (grad\, \boldsymbol{V}) \quad and \quad \boldsymbol{L^T} = (grad\, \boldsymbol{V})^{\boldsymbol{T}}, \tag{3.3}$$

and

$$\boldsymbol{A_1} = grad\, \boldsymbol{V} + (grad\, \boldsymbol{V})^{\boldsymbol{T}} = \boldsymbol{L} + \boldsymbol{L^T}. \tag{3.4}$$

For incompressible movement, the constitutive equations are defined as follows,

$$div.\boldsymbol{V} = 0, \tag{3.5}$$

and

$$\rho \frac{d\boldsymbol{V}}{dt} = div.\boldsymbol{\tau} + \rho \boldsymbol{b}. \tag{3.6}$$

Assuming that a velocity field $\boldsymbol{V}$ and a specific type of extra stress tensor $\boldsymbol{S}$,

$$\boldsymbol{V} = \boldsymbol{V}(y,t) = u(y,t)\hat{\imath}, \quad \boldsymbol{S} = \boldsymbol{S}(y,t), \tag{3.7}$$

Using Eq.$(3.7)_a$ into Eqs. $(3.3) - (3.4)$, we have

$$\boldsymbol{L} = \begin{bmatrix} 0 & \frac{\partial u}{\partial y} & 0 \\ 0 & 0 & 0 \\ 0 & 0 & 0 \end{bmatrix} \quad and \quad \boldsymbol{L^T} = \begin{bmatrix} 0 & 0 & 0 \\ \frac{\partial u}{\partial y} & 0 & 0 \\ 0 & 0 & 0 \end{bmatrix}, \tag{3.8}$$

and

$$\boldsymbol{A_1} = \begin{bmatrix} 0 & \frac{\partial u}{\partial y} & 0 \\ 0 & 0 & 0 \\ 0 & 0 & 0 \end{bmatrix} + \begin{bmatrix} 0 & 0 & 0 \\ \frac{\partial u}{\partial y} & 0 & 0 \\ 0 & 0 & 0 \end{bmatrix} = \begin{bmatrix} 0 & \frac{\partial u}{\partial y} & 0 \\ \frac{\partial u}{\partial y} & 0 & 0 \\ 0 & 0 & 0 \end{bmatrix}. \tag{3.9}$$

Suppose that the fluid is at rest at $t = 0$, and then,

$$u(y, 0) = 0, \qquad s(y, 0) = 0. \tag{3.10}$$

Therefore, Eq. (3.2) becomes

$$\frac{D\boldsymbol{S}}{Dt} = \begin{bmatrix} \frac{\partial}{\partial t}S_{xx} - 2S_{xy}\frac{\partial u}{\partial y} & \frac{\partial}{\partial t}S_{xy} - S_{yy}\frac{\partial u}{\partial y} & \frac{\partial}{\partial t}S_{xz} - S_{yz}\frac{\partial u}{\partial y} \\ \frac{\partial}{\partial t}S_{yx} - S_{yy}\frac{\partial u}{\partial y} & \frac{\partial}{\partial t}S_{yy} & \frac{\partial}{\partial t}S_{yz} \\ \frac{\partial}{\partial t}S_{zx} - S_{zy}\frac{\partial u}{\partial y} & \frac{\partial}{\partial t}S_{zy} & \frac{\partial}{\partial t}S_{zz} \end{bmatrix}, \tag{3.11}$$

Since $S_{xx} = S_{yy} = S_{zz} = S_{xz} = 0$, so that,

$$\frac{D\boldsymbol{S}}{Dt} = \begin{bmatrix} -2S_{xy}\frac{\partial u}{\partial y} & \frac{\partial}{\partial t}S_{xy} & 0 \\ \frac{\partial}{\partial t}S_{yx} & 0 & 0 \\ 0 & 0 & 0 \end{bmatrix}. \tag{3.12}$$

Eq. $(3.1)_b$ becomes.

$$\begin{bmatrix} 0 & S_{xy} & 0 \\ S_{yx} & 0 & 0 \\ 0 & 0 & 0 \end{bmatrix} + \lambda_1 \begin{bmatrix} -2S_{xy}\frac{\partial u}{\partial y} & \frac{\partial}{\partial t}S_{xy} & 0 \\ \frac{\partial}{\partial t}S_{yx} & 0 & 0 \\ 0 & 0 & 0 \end{bmatrix} = \mu \begin{bmatrix} 0 & \frac{\partial u}{\partial y} & 0 \\ \frac{\partial u}{\partial y} & 0 & 0 \\ 0 & 0 & 0 \end{bmatrix}. \tag{3.13}$$

By using Eq. (3.13) into Eq. $(3.1)_a$ and keeping in mind the Eq. (3.10), we get

$$\left(1+\lambda_1\frac{\partial}{\partial t}\right)\tau(y,t)=\mu\frac{\partial u\,(y,t)}{\partial y}. \tag{3.14}$$

When there is no body force, the linear momentum balance Eq. (3.6) decreases to

$$\frac{\partial\tau(y,t)}{\partial t}-\frac{\partial p}{\partial x}=\rho\frac{\partial u(y,t)}{\partial t}. \tag{3.15}$$

By eliminating τ among (3.14) and (3.15), we get

$$\left(1+\lambda_1\frac{\partial}{\partial t}\right)\frac{\partial u}{\partial t}=-\frac{1}{\rho}\left(1+\lambda_1\frac{\partial}{\partial t}\right)\frac{\partial p}{\partial x}+\nu\frac{\partial^2\,u(y,t)}{\partial^2 y};\qquad y,t>0, \tag{3.16}$$

in which $\nu=\frac{\mu}{\rho}$ is a kinematic viscosity. The governing partial differential Eq. (3.16)for an incompressible Maxwell fluid executing the same movement when there's no distinction in pressure.

$$\left(1+\lambda_1\frac{\partial}{\partial t}\right)\frac{\partial u}{\partial t}=\nu\frac{\partial^2 u}{\partial^2 y}. \tag{3.17}$$

As defined, the initial and boundary conditions are;

I.C $$u(y,0)=\frac{\partial u(y,0)}{\partial t}=0,\ and\ \ \tau(y,0)=0,\quad y>0, \tag{3.18}$$

B. C $$u(0,t)=UH(t)sin\omega t\quad or\quad UH(t)cos\omega t\ \ t\geq 0, \tag{3.19}$$

and

$$u(y,t),\ \ \frac{\partial u(y,t)}{\partial y}\to 0\ as\ y\to\infty\ \ and\qquad t>0, \tag{3.20}$$

here, $H(t)$ represents the Heaviside function.

3.3 Calculation of the Velocity Field

3.3.1 Case $-I: UH(t)sin\omega t$

To find the solution to governing Eq. (3.17) and keeping in mind initial and boundary conditions (3.18), $(3.19)_a$ and (3.20), the Fourier sine transform in relation to the spatial variable is applied. Thus, multiplying Eq. (3.17) by $\sqrt{2/\pi}\, sin(y\xi)$, integrating the result from 0 to ∞ with respect to y, we obtain.

$$\frac{\partial u_s(\xi,t)}{\partial t} + \lambda_1 \frac{\partial^2 u_s(\xi,t)}{\partial^2 t} = -\nu\xi^2 u_s(\xi,t) + \sqrt{2/\pi}\, \nu\xi UH sin\omega t, \tag{3.21}$$

where $u_s(\xi,t)$ is the Fourier sine transform of $u(y,t)$, and it must satisfy the following conditions.

$$u_s(\xi,0) = \frac{\partial u_s(\xi,0)}{\partial t} = 0, \quad \xi > 0. \tag{3.22}$$

Moreover, using the Laplace transformation on Eq. (3.21) and using the initial condition (3.22), we find that;

$$\bar{u}_s(\xi,q) = \sqrt{2/\pi}\, \frac{U\nu\xi\omega}{(q^2+\omega^2)[\lambda_1 q^2+q+\nu\xi^2]}\ . \tag{3.23}$$

Now, we modify Eq. (3.23) in the following form.

$$\bar{u}_s(\xi,q) = \frac{U\omega}{\xi}\sqrt{2/\pi}\left\{\frac{1}{(q^2+\omega^2)} - \frac{q(1+\lambda_1 q)}{(q^2+\omega^2)[\lambda_1 q^2+q+\nu\xi^2]}\right\}. \tag{3.24}$$

By using inverse Fourier sine transform, Eq. (3.24), becomes,

$$\bar{u}_s(y,q) = \frac{2U\omega}{\pi}\int_0^\infty \frac{sin(y\xi)}{\xi}\left[\frac{1}{(q^2+\omega^2)} - \frac{q(1+\lambda_1 q)}{(q^2+\omega^2)[\lambda_1 q^2+q+\nu^{\ 2}]}\right] d\xi, \tag{3.25}$$

Now, inverting Eq. (3.25) by means of Laplace transform, we have

$$u_s(y,t) = UH(t)\sin\omega t - \frac{2U\ (t)\omega}{\pi\lambda_1(q_1-q_2)}\int_0^\infty \int_0^t \frac{sin(y\xi)}{\xi} cos\,\omega(t-u) \times \{(1+\lambda_1 q_1)e^{q_1 u} - (1+\lambda_1 q_2)e^{q_2 u})\}d\xi du, \quad (3.26)$$

where,

$$q_1, q_2 = -\frac{(1)\pm\sqrt{1\ -4\lambda_1(\nu\xi^2\ )}}{2\lambda}, \quad (3.27)$$

are the roots of $\lambda_1 q^2 + q + \nu\xi^2 = 0$.

3.3.2 Case $-II : UH(t)cos\omega t$

To find the solution to governing Eq. (3.17) and keeping in mind initial and boundary conditions (3.18), (3.19)b and (3.20), the Fourier sine transform in relation to the spatial variable is applied. Thus, multiplying Eq.(3.17) by $\sqrt{2/\pi}\ sin(y\xi)$, integrating the outcome from 0 to ∞ with respect to y, we obtain;

$$\frac{\partial u_s(\xi,t)}{\partial t} + \lambda_1 \frac{\partial^2 u_s(\xi,t)}{\partial^2 t} = -\nu\xi^2\, u_s(\xi,t) + \sqrt{2/\pi}\ \nu\xi UHcos\omega t, \quad (3.28)$$

where $u_s(\xi,t)$ is the Fourier sine transform of $u(y,t)$, and it must satisfy the following conditions;

$$u_s(\xi,0) = \frac{\partial\, u_s\ (\xi,0)}{\partial t} = 0, \quad \xi > 0. \quad (3.29)$$

Moreover, applying the Laplace transform on Eq. (3.28) and by means of the initial condition (3.18), we find that;

$$\bar{u}_s(\xi,q) = \sqrt{2/\pi}\ \frac{U\nu\xi q}{(q^2+\omega^2)[\lambda_1 q^2+q+\nu\xi^2]}. \quad (3.30)$$

Now, we modify Eq. (3.30) in the following form;

$$\bar{u}_s(\xi, q) = \frac{Uq}{\xi}\sqrt{2/\pi}\left\{\frac{1}{(q^2+\omega^2)} - \frac{q(1+\lambda_1 q)}{(q^2+\omega^2)[\lambda_1 q^2+q+\nu\xi^2]}\right\}. \tag{3.31}$$

By using the inverse Fourier sine transform, Eq. (3.31) becomes,

$$\bar{u}_s(y, q) = \frac{2Uq}{\pi}\int_0^\infty \frac{sin(y\xi)}{\xi}\left[\frac{1}{(q^2+\omega^2)} - \frac{q(1+\lambda_1 q)}{(q^2+\omega^2)[\lambda_1 q^2+q+\nu\xi^2]}\right] d\xi. \tag{3.32}$$

Inverting Eq. (3.32) by means of Laplace transform, we have

$$u_c(y,t) = UH(t)\cos\omega t - \frac{2UH(t)\omega}{\pi\lambda_1(q_1-q_2)}\int_0^\infty\int_0^t \frac{sin(y\xi)}{\varepsilon} sin\,\omega(t-u) \times \{(1+\lambda_1 q_1)e^{q_1 u} - (1+\lambda_1 q_2)e^{q_2 u})\} d\xi du. \tag{3.33}$$

where, q_1 and q_2 are the same given in Eq. (3.27).

3.4 Calculations of the Shear Stress

3.4.1 Case $-I: UH(t)sin\omega t$

By applying the Laplace transform to the Eq. (3.14), we get

$$\bar{\tau}(y, q) = \frac{\mu}{(1+\lambda_1 q)}\frac{\partial \bar{u}(y,q)}{\partial y}, \tag{3.34}$$

where Laplace transform of $\tau(y,t)$ is $\bar{\tau}(y,q)$. Now, differentiate Eq. (3.25) w.r.t 'y', we obtain

$$\frac{\partial \bar{u}(y,q)}{\partial y} = \frac{2U\omega}{\pi}\int_0^\infty cos(y\xi)\left[\frac{1}{(q^2+\omega^2)} - \frac{q(1+\lambda_1 q)}{(q^2+\omega^2)[\lambda_1 q^2+q+\nu\xi^2]}\right] d\xi. \tag{3.35}$$

Using Eq. (3.35) into Eq. (3.34), we get

$$\bar{\tau}(y,q) = \frac{\mu}{(1+\lambda_1 q)}\left[\frac{2U\omega}{\pi}\int_0^\infty cos(y\xi)\left\{\frac{1}{(q^2+\omega^2)} - \frac{q(1+\lambda_1 q)}{(q^2+\omega^2)[\lambda_1 q^2+q+\nu\xi^2]}\right\}d\xi\right], \tag{3.36}$$

and after simplification above Eq. (3.36) becomes

$$\bar{\tau}(y,q) = \frac{2U\omega\mu}{\pi}\int_0^\infty cos(y\xi)\left[\frac{1}{(q^2+\omega^2)(1+\lambda_1 q)} - \frac{q}{(q^2+\omega^2)[\lambda_1 q^2+q+\nu\xi^2]}\right]d\xi. \tag{3.37}$$

Applying the inverse Laplace transform to Eq. (3.37), we get

$$\tau_s\,(y,t) = -\frac{2UH(t)\omega\mu}{\pi\lambda_1(q_1-q_2)}\int_0^\infty\int_0^t cos(y\xi)\,cos\omega(t-u)\,(e^{q_1 u} - e^{q_2 u})d\xi du. \tag{3.38}$$

3.4.2 Case $-II$: $UH(t)\,cos\,\omega t$

Similarly, differentiate Eq. (3.32) w.r.t y, we get

$$\frac{\partial\bar{u}(y,q)}{\partial y} = \frac{2Uq}{\pi}\int_0^\infty cos(y\xi)\left[\frac{1}{(q^2+\omega^2)} - \frac{q(1+\lambda_1 q)}{(q^2+\omega^2)[\lambda_1 q^2+q+\nu\xi^2]}\right]d\xi. \tag{3.39}$$

Substitute above Eq. (3.39) into Eq. (3.34), we obtain

$$\bar{\tau}(y,q) = \frac{\mu}{(1+\lambda_1 q)}\left[\frac{2Uq}{\pi}\int_0^\infty cos(y\xi)\left\{\frac{1}{(q^2+\omega^2)} - \frac{q(1+\lambda_1 q)}{(q^2+\omega^2)[\lambda_1 q^2+q+\nu\xi^2]}\right\}d\xi\right]. \tag{3.40}$$

After simplification Eq. (3.40) becomes

$$\bar{\tau}(y,q) = \frac{2Uq\mu}{\pi}\int_0^\infty cos(y\xi)\left[\frac{1}{(q^2+\omega^2)(1+\lambda_1 q)} - \frac{q}{(q^2+\omega^2)[\lambda_1 q^2+q+\nu\xi^2]}\right]d\xi. \tag{3.41}$$

Finally, applying inverse Laplace transform to Eq. (3.41), we get

$$\tau_c\,(y,t) = -\frac{2UH(t)\omega\mu}{\pi\lambda_1(q_1-q_2)}\int_0^\infty\int_0^t cos(y\xi)\,sin\omega(t-\,u)\,(e^{q_1 u}-e^{q_2 u})d\xi du. \qquad (3.42)$$

3.5 Limiting Case: A Newtonian Fluid ($\lambda_1 \to 0$)

When evaluating the limit $\lambda_1 \to 0$ into Eqs. (3.26), (3.33), (3.38) and (3.42), we obtain a similar solution of velocity field and shear stress for Newtonian fluid [42].

$$U_{SN} = UH(t)\,sin\,\omega t - \frac{2UH(t)\omega}{\pi}\int_0^\infty\int_0^t \frac{sin(y\xi)}{\xi} cos\,\omega(t-u)\,e^{-\nu\xi^2}d\xi du, \qquad (3.43)$$

$$U_{CN} = UH(t)\,cos\,\omega t - \frac{2UH(t)\omega}{\pi}\int_0^\infty\int_0^t \frac{sin(y\xi)}{\xi} sin\,\omega(t-u)\,e^{-\nu\xi^2}d\xi du, \qquad (3.44)$$

$$\tau_{SN}\,(y,t) = -\frac{2U\ \ (t)\omega\mu}{\pi}\int_0^\infty\int_0^t cos(y\xi)\,cos\omega(t-u)\ e^{-\nu\xi^2}d\xi du, \qquad (3.45)$$

and

$$\tau_{CN}\,(y,t) = -\frac{2UH(t)\omega\mu}{\pi}\int_0^\infty\int_0^t cos(y\xi)\,sin\omega(t-\,u)\ e^{-\nu\xi^2}d\xi du. \qquad (3.46)$$

3.6 Results and Discussions

To produce comprehensive graphical results pertaining to the problem, numerous computer calculations have been carried out. The solutions for an oscillating flow of an incompressible Maxwell fluid across a flat plate are provided in this chapter. The movement in the fluid is caused by plate oscillation. For the Maxwell fluid across an oscillating plate, using integral transform techniques (Fourier sine and Laplace transforms), the governing partial differential equations are solved to find the solution. These results fulfill all initial and boundary conditions. When $\lambda_1 \to 0$ executing the comparable motion, the generic Solutions for the motion of a Newtonian fluid are simplified and made more specific. Detailed graphs are used to demonstrate the numerical findings for the velocity profile $u(y,t)$ and the accompanying shear stress $\tau(y,t)$ are plotted in Figures $3.1 - 3.4$. We examine these findings in relation to the variations of the time parameter t , frequency ω, relaxation time parameter λ_1, and kinematic viscosity ν.

Figure 3.1 shows the influence of different values of time t for $t = 0.1, 0.2, 0.3$ and 0.5 on velocity profile obtained in Eq. (3.26) and corresponding shear stress of Eq. (3.38), respectively. In both cases, velocity profile and shear stress increase with respect to time t from maximum values to zero values. Figure 3.2 shows the influence of relaxation time parameter at $\lambda_1 = 1.0, 1.5, 2.0$ and 4.0 on velocity profile and shear stress correspondingly. Shear stress and the velocity profile both reduce from maximum values to zero values in both situations. For viscoelasticity, the relaxation time has a point where the fluid's motion intersects. Figure 3.3 shows the influence of kinematic viscosity ν at different values of ν i.e. $\nu = 0.1, 0.2, 0.3$ and 0.4 on the velocity profile and shear stress respectively. In both cases, velocity profile and shear stress increases from maximum values to zero values and clearly satisfies boundary conditions. It should be observed that, with regard to kinematic viscosity v, the fluid's velocity field is increasing function along with the shear stress. Figure 3.4 shows the influence of the frequency parameter ω for $\omega = 1.0, 1.1, 1.3$ and 1.5 on the velocity profile and shear stress respectively. It should be noted that velocity profile along with shear stress is an increasing function.

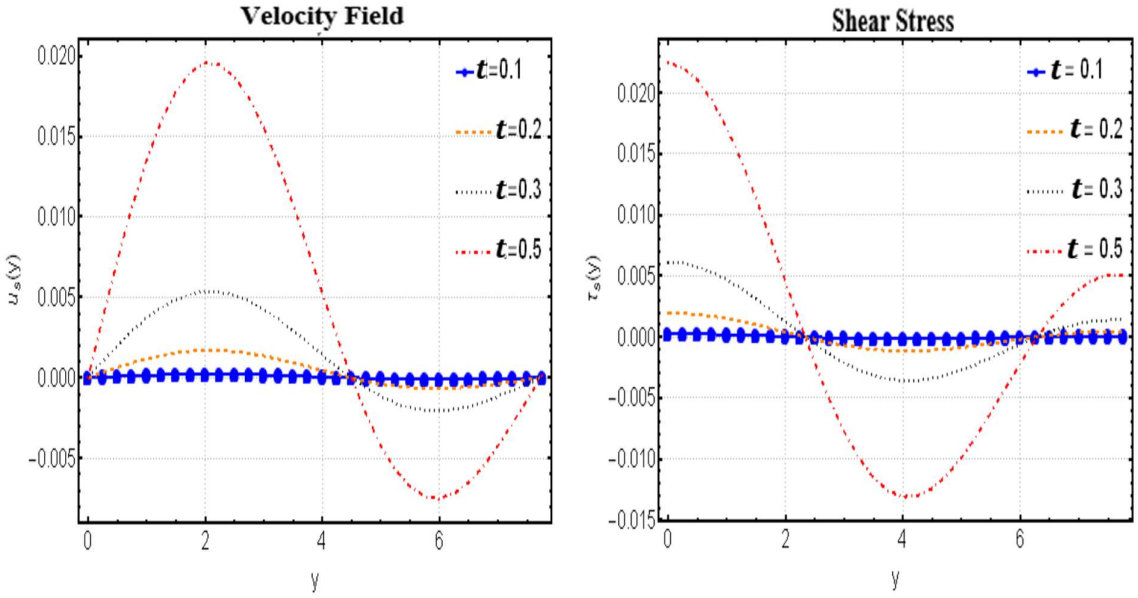

Fig. 3.1. Profile of the velocity field $u_s(y,t)$ and the shear stress $\tau_s(y,t)$ for $U=1$, $\nu=2$, $\lambda_1=2$, $\omega=5$ and diverse values t.

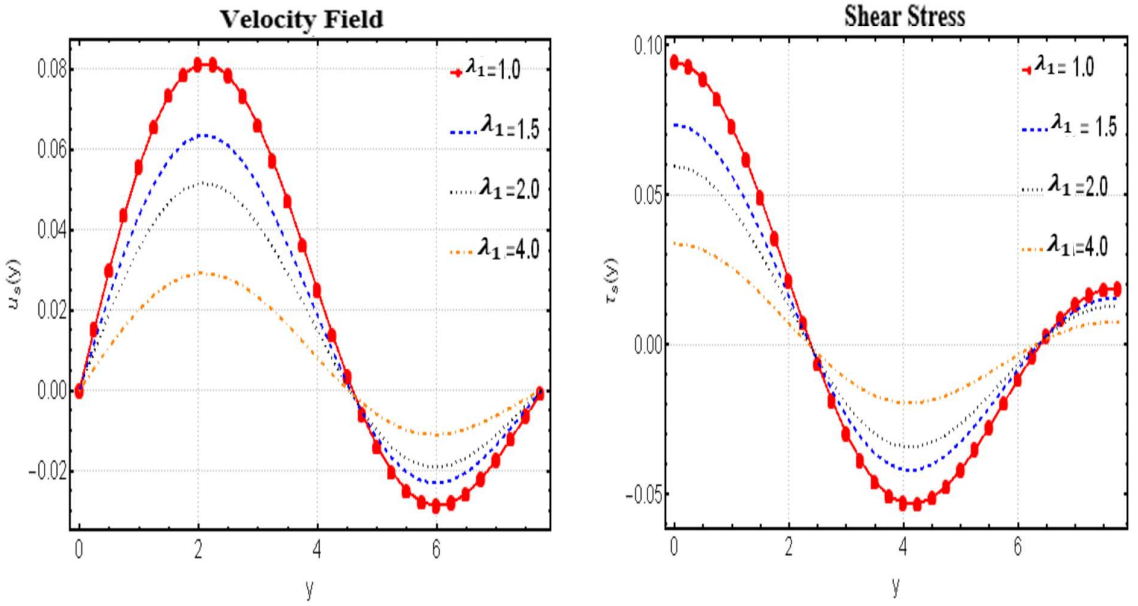

Fig. 3.2. Profile of the velocity field $u_s(y,t)$ and the shear stress $\tau_s(y,t)$ for $U=1$, $\nu=2$, $t=1$, $\omega=5$ and diverse values λ_1.

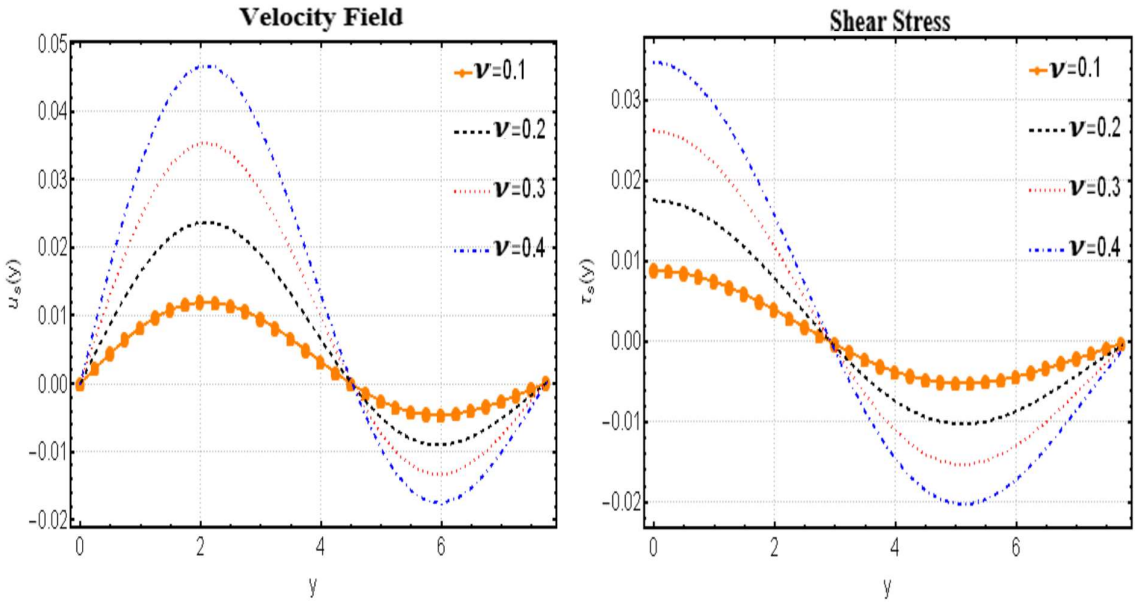

Fig. 3.3. Profile of the velocity field $u_s(y,t)$ and the shear stress $\tau_s(y,t)$ for $U=1$, $\lambda_1=2$, $t=2$, $\omega=2$ and changed values of ν.

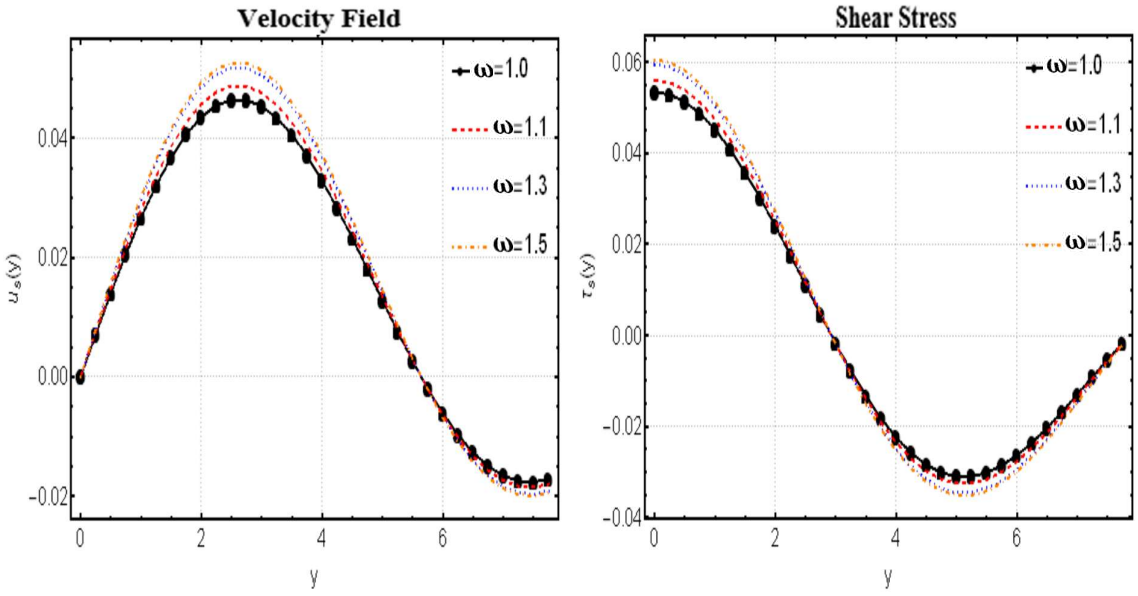

Fig. 3.4. The profile of the velocity field $u_s(y,t)$ and the shear stress $\tau_s(y,t)$ for $U=1$, $\lambda_1=2$, $t=2$, $\nu=0.63$ as well as dissimilar values of ω.

CHAPTER 4

Exact Solutions for Oldroyd-B Fluid over an Oscillating Plate

4.1 Introduction

In this chapter, the exact solutions for Oldroyd-B fluid over an oscillating plate is observed. The solutions for the velocity field $u(y,t)$ and the shear stress $\tau(y,t)$ for the Oldroyd-B fluid are derived using integral transforms, specifically Fourier sine and Laplace transforms. The terms $\tau(y,t)$ for shear stress and $u(y,t)$ for the velocity field, fulfill each and every initial and boundary conditions. To represent different physical scenarios, we created graphical representations using various combinations of variables. After collecting and examining the data, we conducted a comparative analysis to understand the results better. This analysis showed that our findings align well with the results of previous research, confirming the validity and reliability of the study.

4.2 Geometry of the Problem

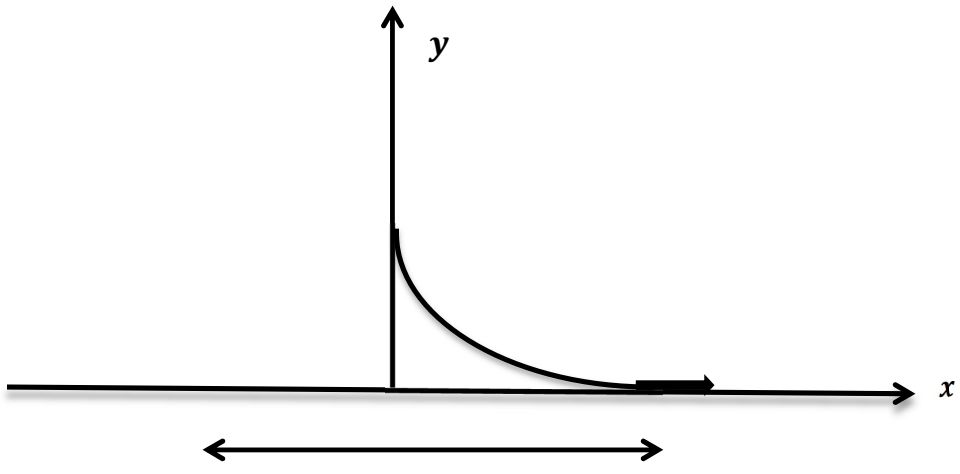

Fig 4.1: Geometry of the problem

4.3 Mathematical Formulation

Suppose the area that lies over the surface of a plate that is perpendicular to y −axis is filled with an incompressible Oldroyd-B fluid. The liquid is at rest when $t \leq 0$, and the surface of the plate is suddenly caused by a constant velocity U in its own plane at $t = 0^+$. The liquid is transferred slowly and gradually above the plate as a result of shear stress. For the Oldroyd-B fluid over a fluctuating plate, the outcomes are found by solving the differential equations that govern via the integral changes approach (Fourier sine and Laplace transform). The Cauchy's stress tensor in an Oldroyd-B fluid is of the following form;

$$\boldsymbol{T} = -p\boldsymbol{I} + \boldsymbol{S}, \quad \boldsymbol{S} + \lambda_1 \frac{\boldsymbol{DS}}{\boldsymbol{Dt}} = \mu \boldsymbol{A_1} + \mu\lambda_2 \frac{\boldsymbol{DA_1}}{\boldsymbol{Dt}}, \tag{4.1}$$

in which $\boldsymbol{T}$ is the Cauchy stress tensor, $-p\boldsymbol{I}$ represents the unknown spherical stress, $\boldsymbol{S}$ is the extra stress tensor, λ_1 is the relaxation time, λ_2 is the retardation time, μ is the viscosity, $\boldsymbol{A_1}$ is the first Rivlin Ericksen tensor and $\frac{D}{Dt}$ is upper convective derivative defined below

$$\frac{\boldsymbol{DS}}{\boldsymbol{Dt}} = \frac{\boldsymbol{dS}}{\boldsymbol{dt}} - \boldsymbol{LS} - \boldsymbol{SL^T}, \tag{4.2}$$

where

$$\boldsymbol{L} = (grad\, \boldsymbol{V}) \quad and \quad \boldsymbol{L^T} = (grad\, \boldsymbol{V})^{\boldsymbol{T}}, \tag{4.3}$$

and

$$\boldsymbol{A_1} = grad\, \boldsymbol{V} + (grad\, \boldsymbol{V})^{\boldsymbol{T}} = \boldsymbol{L} + \boldsymbol{L^T}. \tag{4.4}$$

The flow with incompressible constitutive equations are defined as

$$div.\boldsymbol{V} = 0, \tag{4.5}$$

and

$$\rho \frac{\boldsymbol{dV}}{\boldsymbol{dt}} = div.\boldsymbol{\tau} + \rho \boldsymbol{b}. \tag{4.6}$$

Assuming that a velocity field $\boldsymbol{V}$ and an extra stress tensor $\boldsymbol{S}$ of a particular method,

$$\boldsymbol{V} = \boldsymbol{V}(y,t) = u(y,t)\hat{\imath}, \qquad \boldsymbol{S} = \boldsymbol{S}(y,t). \tag{4.7}$$

Using Eq. $(4.7)_a$ into Eqs. $(4.3) - (4.4)$, we have

$$\boldsymbol{L} = \begin{bmatrix} 0 & \frac{\partial u}{\partial y} & 0 \\ 0 & 0 & 0 \\ 0 & 0 & 0 \end{bmatrix} \quad \text{and} \quad \boldsymbol{L^T} = \begin{bmatrix} 0 & 0 & 0 \\ \frac{\partial u}{\partial y} & 0 & 0 \\ 0 & 0 & 0 \end{bmatrix}, \tag{4.8}$$

and

$$\boldsymbol{A_1} = \begin{bmatrix} 0 & \frac{\partial u}{\partial y} & 0 \\ 0 & 0 & 0 \\ 0 & 0 & 0 \end{bmatrix} + \begin{bmatrix} 0 & 0 & 0 \\ \frac{\partial u}{\partial y} & 0 & 0 \\ 0 & 0 & 0 \end{bmatrix} = \begin{bmatrix} 0 & \frac{\partial u}{\partial y} & 0 \\ \frac{\partial u}{\partial y} & 0 & 0 \\ 0 & 0 & 0 \end{bmatrix}. \tag{4.9}$$

Suppose that the fluid is at rest at $t = 0$, and then,

$$u(y,0) = 0, \qquad S(y,0) = 0. \tag{4.10}$$

Therefore, Eq. (4.2) becomes

$$\frac{D\boldsymbol{S}}{Dt} = \begin{bmatrix} \frac{\partial}{\partial t}S_{xx} - S_{xy}\frac{\partial u}{\partial y} & \frac{\partial}{\partial t}S_{xy} - S_{yy}\frac{\partial u}{\partial y} & \frac{\partial}{\partial t}S_{xz} - S_{yz}\frac{\partial u}{\partial y} \\ \frac{\partial}{\partial t}S_{yx} - S_{yy}\frac{\partial u}{\partial y} & \frac{\partial}{\partial t}S_{yy} & \frac{\partial}{\partial t}S_{yz} \\ \frac{\partial}{\partial t}S_{zx} - S_{zy}\frac{\partial u}{\partial y} & \frac{\partial}{\partial t}S_{zy} & \frac{\partial}{\partial t}S_{zz} \end{bmatrix}. \tag{4.11}$$

Since $S_{xx} = S_{yy} = S_{zz} = S_{xz} = 0$, so that,

$$\frac{D\boldsymbol{S}}{Dt} = \begin{bmatrix} -2S_{xy}\frac{\partial u}{\partial y} & \frac{\partial}{\partial t}S_{xy} & 0 \\ \frac{\partial}{\partial t}S_{yx} & 0 & 0 \\ 0 & 0 & 0 \end{bmatrix}. \tag{4.12}$$

Eq. $(4.1)_b$ becomes;

$$\begin{bmatrix} 0 & S_{xy} & 0 \\ S_{yx} & 0 & 0 \\ 0 & 0 & 0 \end{bmatrix} + \lambda_1 \begin{bmatrix} -2S_{xy}\frac{\partial u}{\partial y} & \frac{\partial}{\partial t}S_{xy} & 0 \\ \frac{\partial}{\partial t}S_{yx} & 0 & 0 \\ 0 & 0 & 0 \end{bmatrix} = \mu \begin{bmatrix} 0 & \frac{\partial u}{\partial y} & 0 \\ \frac{\partial u}{\partial y} & 0 & 0 \\ 0 & 0 & 0 \end{bmatrix} + \mu\lambda_2 \begin{bmatrix} 0 & \frac{\partial^2 u}{\partial y \partial t} & 0 \\ \frac{\partial^2 u}{\partial y \partial t} & 0 & 0 \\ 0 & 0 & 0 \end{bmatrix}. \tag{4.13}$$

By using Eq. (4.13) into Eq. $(4.1)_a$ and keeping in mind the Eq. (4.10), we get

$$\left(1 + \lambda_1 \frac{\partial}{\partial t}\right)\tau(y,t) = \mu\left(1 + \lambda_2 \frac{\partial}{\partial t}\right)\frac{\partial u\,(y,t)}{\partial y}. \tag{4.14}$$

When there is no body force, The state of balance of Eq. (4.6) linear momentum reduces to

$$\frac{\partial \tau(y,t)}{\partial y} - \frac{\partial p}{\partial x} = \rho \frac{\partial u(y,t)}{\partial t}. \tag{4.15}$$

By eliminating τ among Eqs. (4.14) and (4.15), we get

$$\left(1 + \lambda_1 \frac{\partial}{\partial t}\right)\frac{\partial u}{\partial t} = -\frac{1}{\rho}\left(1 + \lambda_1 \frac{\partial}{\partial t}\right)\frac{\partial p}{\partial x} + \nu\left(1 + \lambda_2 \frac{\partial}{\partial t}\right)\frac{\partial^2\, u(y,t)}{\partial^2 y}; y, t > 0, \tag{4.16}$$

in which $\nu = \frac{\mu}{\rho}$, a kinematic viscosity. The governing partial differential Eq. (4.16) for an incompressible Oldroyd-B fluid executing the same motion in the absence of a pressure gradient;

$$\left(1 + \lambda_1 \frac{\partial}{\partial t}\right)\frac{\partial u}{\partial t} = \nu\left(1 + \lambda_2 \frac{\partial}{\partial t}\right)\frac{\partial^2 u}{\partial^2 y}. \tag{4.17}$$

The initial and boundary conditions are defined as:

I.C $$u(y,0) = \frac{\partial u(y,0)}{\partial t} = 0, \text{ and } \tau(y,0) = 0, \quad y > 0, \tag{4.18}$$

B.C $$u(0,t) = UH(t)sin\omega t \quad or \quad UH(t)cos\omega t \;\; t \geq 0, \tag{4.19}$$

and

$$u(y,t),\ \ \frac{\partial u(y,t)}{\partial y} \to 0\ as\ y \to \infty\ \ and\ \ t > 0, \tag{4.20}$$

where $H(t)$ represents the Heaviside function.

4.4 Calculation of the Velocity Field

4.4.1 Case $-I : UH(t)sin\omega t$

To find the solution to governing Eq.(4.17) and considering the initial and boundary conditions (4.18), $(4.19)_a$ and (4.20), the Fourier sine transform in relation to the spatial variable is applied. Thus, multiplying Eq.(4.17) by $\sqrt{2/\pi}\ sin(y\xi)$, integrating the result from 0 to ∞ with respect to y, we obtain;

$$\frac{\partial u_s(\xi,t)}{\partial t} + \lambda_1 \frac{\partial^2 u_s(\xi,t)}{\partial^2 t} = -\nu\xi^2 u_s(\xi,t) + \sqrt{2/\pi}\ \nu\xi UHsin\omega t - \nu\xi^2\lambda_2 \frac{\partial}{\partial t}u_s(\mathrm{E},t) + \sqrt{2/\pi}\,\xi U\lambda_2 \frac{\partial}{\partial t}H(t)sin\omega t, \tag{4.21}$$

where $u_s(\xi,\mathrm{t})$ is the Fourier sine transform of $u(y,t)$, and it must satisfy the following conditions;

$$u_s(\xi,0) = \frac{\partial\, u_s\ (\xi,0)}{\partial t} = 0, \qquad \xi > 0. \tag{4.22}$$

Moreover, applying the Laplace transform on Eq. (4.21) and applying the initial condition (4.22) in, we find that;

$$\bar{\mathrm{u}}_s(\xi,q) = \sqrt{2/\pi}\ \left\{\frac{U\nu\xi\omega}{(q^2+\omega^2)[\lambda_1 q^2+q(1+\nu\xi^2\lambda_2)+\nu\xi^2]} + \frac{U\nu\xi q\lambda_2}{(q^2+\omega^2)[\lambda_1 q^2+q(1+\nu\xi^2\lambda_2)+\nu\xi^2]}\right\}. \tag{4.23}$$

Now, we modify Eq. (4.23) in the following form;

$$\bar{u}_s(\xi, q) = \frac{U\omega}{\xi}\sqrt{2/\pi}\left\{\frac{1}{(q^2+\omega^2)} - \frac{\lambda_1 q^2 + A\lambda_2 q}{(q^2+\omega^2)[\lambda_1 q^2 + q((1+\nu\xi^2\lambda_2)+\nu\xi^2]}\right\}, \tag{4.24}$$

where

$$A = \left[1 + (1 - \frac{1}{\omega})\nu\xi^2\right].$$

By using the inverse Fourier transform, Eq. (4.24) becomes,

$$\bar{u}_s(y, q) = \frac{2U\omega}{\pi}\int_0^\infty \frac{sin(y\xi)}{\xi}\left[\frac{1}{(q^2+\omega^2)} - \frac{\lambda_1 q^2 + A\lambda_2 q}{(q^2+\omega^2)[\lambda_1 q^2 + q((1+\nu\xi^2\lambda_2)+\nu\xi^2]}\right]. \tag{4.25}$$

Now, inverting Eq. (4.25) by means of Laplace transform, we have

$$u_s(y,t) = UH(t)\,sin\,\omega t - \frac{2UH(t)\omega}{\pi\lambda_1(q_1-q_2)}\int_0^\infty\int_0^t \frac{sin(y\xi)}{\xi} cos\,\omega(t-u)\times \{(\lambda_1 q_1 + A\lambda_2)e^{q_1 u} - (\lambda_1 q_2 + A\lambda_2)e^{q_2 u})\}d\xi du, \tag{4.26}$$

where

$$q_1, q_2 = \frac{(-1-\lambda_2\nu\xi)\pm\sqrt{(1+\lambda_2\nu\xi)^2 - 4\lambda_1\nu\xi^2}}{2\lambda_1}, \tag{4.27}$$

are the roots of the algebraic expression $\lambda_1 q^2 + q(1 + \nu\xi^2\lambda_2) + \nu\xi^2 = 0$.

4.4.2 Case $-II : UH(t)cos\omega t$

To find the solution of governing Eq. (4.17) and taking into account both the initial and boundary conditions (4.18) , (4.19)b and (4.20) , the spatial variable is taken into consideration while applying the Fourier sine transform. Thus, multiplying Eq. (4.17) by $\sqrt{2/\pi}\,sin(y\xi)$, integrating the result from 0 to ∞ with respect to y, we obtain;

$$\frac{\partial u_s(\xi,t)}{\partial t} + \lambda_1\frac{\partial^2 u_s(\xi,t)}{\partial^2 t} = -\nu\xi^2 u_s(\xi,t) + \sqrt{2/\pi}\,\nu\xi UHcos\omega t - \nu\xi^2\lambda_2\frac{\partial}{\partial t}u_s(\xi,t) + \sqrt{2/\pi}\,\xi U\lambda_2\frac{\partial}{\partial t}H(t)cos\omega t, \tag{4.28}$$

where $u_s(\xi,t)$ is the Fourier sine transform of $u(y,t)$, and it must satisfy the following conditions;

$$u_s(\xi,0)=\frac{\partial\, u_s\ (\xi,0)}{\partial t}=0, \qquad \xi>0. \tag{4.29}$$

Moreover, applying the Laplace transform on Eq. (4.28) and keeping the initial condition (4.18) in mind, we find that;

$$\bar{\mathrm{u}}_s(\xi,q)=\sqrt{2/\pi}\ \left\{\frac{U\nu\xi q}{(q^2+\omega^2)[\lambda_1 q^2+q(1+\nu\xi^2\lambda_2)+\nu\xi^2]}+\frac{U\nu\xi\omega\lambda_2}{(q^2+\omega^2)[\lambda_1 q^2+q(1+\nu\xi^2\lambda_2)+\nu\xi^2]}\right\}. \tag{4.30}$$

Now, we modify Eq. (4.30) in the following form;

$$\bar{\mathrm{u}}_s(\xi,q)=\frac{Uq}{\xi}\sqrt{2/\pi}\ \left\{\frac{1}{(q^2+\omega^2)}-\frac{\lambda_1 q^2+A\lambda_2 q}{(q^2+\omega^2)[\lambda_1 q^2+q((1+\nu\xi^2\lambda_2)+\nu\xi^2]}\right\}, \tag{4.31}$$

where

$$A=\left[1+(1-\frac{1}{\omega})\nu\xi^2\right].$$

By using inverse Fourier sine transform, Eq. (4.31) becomes,

$$\bar{\mathrm{u}}_s(y,q)=\frac{2Uq}{\pi}\int_0^\infty \frac{sin(y\xi)}{\xi}\left[\frac{1}{(q^2+\omega^2)}-\frac{\lambda_1 q^2+A\lambda_2 q}{(q^2+\omega^2)[\lambda_1 q^2+q((1+\nu\xi^2\lambda_2)+\nu\xi^2]}\right]. \tag{4.32}$$

Now, inverting Eq. (4.32) by means of Laplace transform,

$$u_c(y,t)=UH(t)\,cos\,\omega t-\frac{2UH(t)\omega}{\pi\lambda_1(q_1-q_2)}\int_0^\infty\int_0^t\frac{sin(y\xi)}{\xi}sin\,\omega(t-u)\times$$
$$\{(\lambda_1 q_1+A\lambda_2)e^{q_1 u}-(\lambda_1 q_2+A\lambda_2)e^{q_2 u})\}d\xi du, \tag{4.33}$$

where, q_1 and q_2 are the same given in Eq. (4.27).

4.5 Calculations of the Shear Stress

4.5.1 Case$-I: UH(t)sin\omega t$

By applying Laplace transform to the Eq. (4.14), we get

$$\bar{\tau}(y,q) = \mu\left[\frac{(1+\lambda_2 q)}{(1+\lambda_1 q)}\right]\frac{\partial \bar{u}(y,q)}{\partial y}, \tag{4.34}$$

where Laplace transform of $\tau(y,t)$ is $\bar{\tau}(y,q)$. Now, differentiate Eq. (4.25) w.r.t y,we obtain

$$\frac{\partial \bar{u}(y,q)}{\partial y} = \frac{2U\omega}{\pi}\int_0^\infty cos(y\xi)\left[\frac{1}{(q^2+\omega^2)} - \frac{\lambda_1 q^2+(1+B\lambda_2)q}{(q^2+\omega^2)[\lambda_1 q^2+q((1+\nu\xi^2\lambda_2)+\nu\xi^2]}\right]d\xi, \tag{4.35}$$

where,

$$B = \left(1-\frac{1}{\omega}\nu\xi^2\right).$$

Using Eq. (4.35) in Eq. (4.34), we get

$$\bar{\tau}(y,q) = \mu\left[\frac{(1+\lambda_2 q)}{(1+\lambda_1 q)}\right]\left[\frac{2U}{\pi}\int_0^\infty cos(y\xi)\left\{\frac{1}{(q^2+\omega^2)} - \frac{\lambda_1 q^2+(1+B\lambda_2)q}{(q^2+\omega^2)[\lambda_1 q^2+q((1+\nu\xi^2\lambda_2)+\nu\xi^2]}\right\}d\xi\right], \tag{4.36}$$

and after simplification above Eq. (4.36) becomes

$$\bar{\tau}(y,q) = \frac{2U\omega\mu}{\lambda_1\pi}\int_0^\infty cos(y\xi)\left[\frac{(1+\lambda_2 q)}{(1+\lambda_1 q)}\right]\left[\frac{1}{(q^2+\omega^2)} - \frac{\lambda_1 q^2+(1+B\lambda_2)q}{(q^2+\omega^2)(q-q_1)(q-q_2)}\right]d\xi. \tag{4.37}$$

Applying the inverse Laplace transform to Eq. (4.37), we get

$$\tau_s(y,t) = -\frac{2UH(t)\omega\mu}{\pi\lambda_1}\int_0^\infty\int_0^t cos(y\xi)[cos\omega(t-u)+\lambda_2(\delta(t-u)-\omega sin\omega(t-u))]\times$$
$$\left[\frac{Be^{\frac{-u}{\lambda_1}}\lambda_1\lambda_2}{(1+q_1\lambda_1)(1+q_1\lambda_2)} + \frac{e^{q_1 u}(1+\lambda_1 q_1+A\lambda_2)}{(q_1-q_2)(1+\lambda_1 q_1)} - \frac{e^{q_2 u}(1+\lambda_1 q_2+A\lambda_2)}{(q_1-q_2)(1+\lambda_1 q_2)}\right]d\xi du. \tag{4.38}$$

4.5.2 Case -*II*: $UH(t)\cos\omega t$

Similarly, differentiate Eq. (4.32) w.r.t $'y'$, we get

$$\frac{\partial\bar{u}(y,q)}{\partial y} = \frac{2U}{\pi}\int_0^\infty cos(y\xi)\left[\frac{1}{(q^2+\omega^2)} - \frac{\lambda_1 q^2+(1+B\lambda_2)q}{(q^2+\omega^2)[\lambda_1 q^2+q((1+\nu\xi^2\lambda_2)+\nu\xi^2]}\right]d\xi, \quad (4.39)$$

where,

$$B = \left(1-\frac{1}{\omega}\nu\xi^2\right).$$

And substitute above Eq. (4.39) into Eq. (4.34), we obtain

$$\bar{\tau}(y,q) = \mu\left[\frac{(1+\lambda_2 q)}{(1+\lambda_1 q)}\right]\left[\frac{2U}{\pi}\int_0^\infty cos(y\xi)\left\{\frac{1}{(q^2+\omega^2)} - \frac{\lambda_1 q^2+(1+B\lambda_2)q}{(q^2+\omega^2)[\lambda_1 q^2+q((1+\nu\xi^2\lambda_2)+\nu\xi^2]}\right\}d\xi\right]. \quad (4.40)$$

After simplification Eq. (4.40) becomes

$$\bar{\tau}(y,q) = \frac{2Uq\mu}{\lambda_1\pi}\int_0^\infty cos(y\xi)\left[\frac{(1+\lambda_2 q)}{(1+\lambda_1 q)}\right]\left[\frac{1}{(q^2+\omega^2)} - \frac{\lambda_1 q^2+(1+B\lambda_2)q}{(q^2+\omega^2)(q-q_1)(q-q_2)}\right]d\xi. \quad (4.41)$$

Finally, applying the inverse Laplace transform to Eq. (4.41), we get

$$\tau_c\,(y,t) = -\frac{2UH(t)\omega\mu}{\pi\lambda_1}\int_0^\infty\int_0^t cos(y\xi)[sin\omega(t-u) + \lambda_2(\delta(t-u) - \omega sin\omega(t-u))]\times$$
$$\left[\frac{Be^{\frac{-u}{\lambda_1}}\lambda_1\lambda_2}{(1+q_1\lambda_1)(1+q_1\lambda_2)} + \frac{e^{q_1 u}(1+\lambda_1 q_1+A\lambda_2)}{(q_1-q_2)(1+\lambda_1 q_1)} - \frac{e^{q_2 u}(1+\lambda_1 q_2+B\lambda_2)}{(q_1-q_2)(1+\lambda_1 q_2)}\right]d\xi du. \quad (4.42)$$

4.6 Limiting Case: A Newtonian Fluid ($\lambda_1 \to 0, \lambda_2 \to 0$)

Taking the limit $\lambda_1 \to 0$ and $\lambda_2 \to 0$ into Eqs. (4.26), (4.33), (4.38) and (4.42), we obtain a similar solution of velocity field and hear stress for Newtonian fluid [40].

$$U_{SN} = UH(t)\sin\omega t - \frac{2UH(t)\omega}{\pi}\int_0^\infty \int_0^t \frac{\sin(y\xi)}{\varepsilon}\cos\omega(t-u)\, e^{-\nu\xi^2} d\xi du, \qquad (4.43)$$

$$U_{CN} = UH(t)\cos\omega t - \frac{2UH(t)\omega}{\pi}\int_0^\infty \int_0^t \frac{\sin(y\xi)}{\varepsilon}\sin\omega(t-u)\, e^{-\nu\xi^2} d\xi du, \qquad (4.44)$$

$$\tau_{SN}(y,t) = -\frac{2U\ (t)\omega\mu}{\pi}\int_0^\infty \int_0^t \cos(y\xi)\cos\omega(t-u)\ e^{-\nu\xi^2} d\xi du, \qquad (4.45)$$

and

$$\tau_{CN}(y,t) = -\frac{2UH(t)\omega\mu}{\pi}\int_0^\infty \int_0^t \cos(y\xi)\sin\omega(t-u)\ e^{-\nu\xi^2} d\xi du. \qquad (4.46)$$

4.7 Results and Discussions

In this section, we provide solutions for an oscillating Oldroyd-B flow of an incompressible fluid over a flat plat. Due to plate oscillation causes motion in the fluid. For the Oldroyd-B fluid across an oscillating plate, the solutions are obtained by applying integral transform techniques to solve the governing partial differential equations. These results fulfill each and every initial and boundary conditions. When $\lambda_1 \to 0$ and $\lambda_2 \to 0$ executing the comparable motion, for the motion of the Newtonian fluid, the general solutions are simplified and specified. The numerical results for velocity field $u(y,t)$ and shear stress $\tau(y,t)$ are illustrated through plots in Figures $4.2 - 4.6$. We analyze these results in relation to the variations of the time parameter t, frequency ω, relaxation time parameter λ_1 , retardation time parameter λ_2 and kinematic viscosity ν.

Figure 4.2 shows the influence of different values of time t for $t = 0.1, 0.2, 0.3\ and\ 0.5$ on velocity profile obtained in Eq. (4.26) and corresponding shear stress of Eq. (4.38) respectively. Velocity profile along with shear stress is a function that increases with respect to time t from maximum values to zero values. Figure 4.3 shows the influence of relaxation time parameter at $\lambda_1 = 2$ at different values of retardation time parameter λ_2 for $\lambda_2 = 0.5, 1.0, 1.5$ and 2.0 on velocity profile and shear stress, respectively. Shear stress and the velocity profile both drop from maximum values to zero values in both situations. Figure 4.4 shows the influence of retardation time parameter $\lambda_2 = 2$ at different values of relaxation time parameter λ_1 for $\lambda_1 = 0.5, 1.0, 1.5$ and 2.0 on velocity profile and shear stress respectively. Velocity profile decreases from maximum values to zero values while shear stress increases from maximum values to zero values. Figure 4.5 shows the influence of kinematic viscosity ν at different values of ν i. e $\nu = 0.1, 0.2, 0.3$ and 0.4 on velocity profile and shear stress respectively. In both cases, velocity profile and shear stress increases from maximum values to zero values and clearly satisfy boundary conditions. It is observed that, in relation to kinematic viscosity ν, the fluid's velocity field is increasing function along with the shear stress. Figure 4.6 shows the influence of frequency parameter ω for $\omega = 1.0, 1.1, 1.3$ and 1.5 on profile of velocity along with shear stress. It's observed that the profile of velocity along with shear stress is decreasing function along with frequency ω.

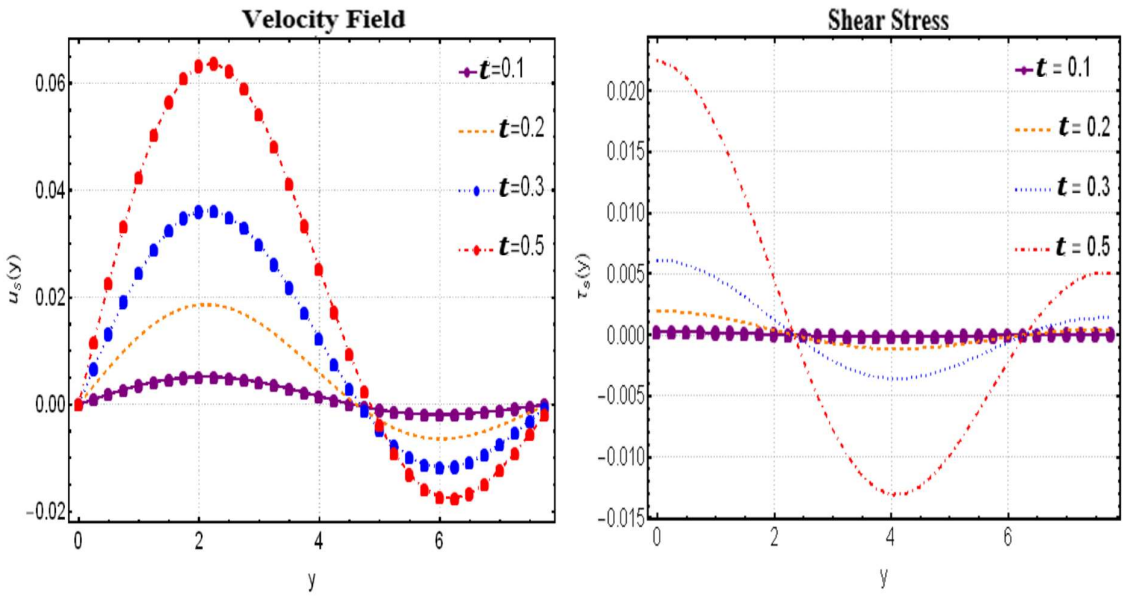

Fig. 4.2. Profile of the velocity field $u_s(y,t)$ and the shear stress $\tau_s(y,t)$ for $U=1, \nu=2$, $\lambda_1=2, \lambda_2=1, \omega=5$ and various points of t.

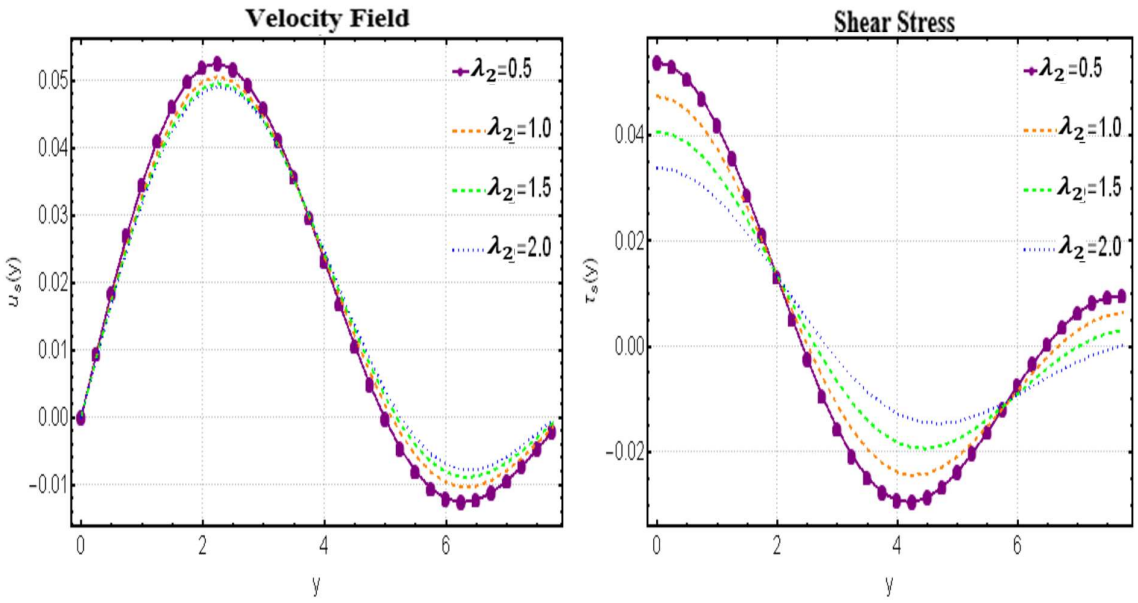

Fig.4.3. Profile of velocity field $u_s(y,t)$ and the shear stress $\tau_s(y,t)$ for $U=1, \nu=2, t=1$, $\omega=5, \lambda_1=2$ and various values of λ_2 .

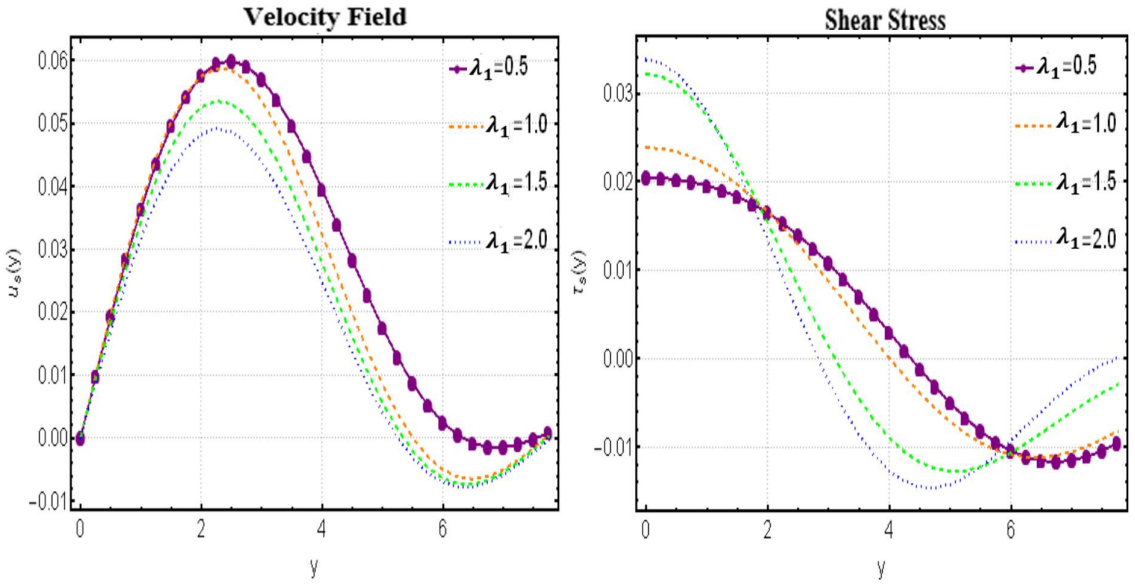

Fig. 4. 4. Profile of the velocity field $u_s(y,t)$ and the shear stress $\tau_s(y,t)$ for $U = 1$, $\nu = 2$, $t = 1$, $\omega = 5$, $\lambda_2 = 2$ and various points of λ_1.

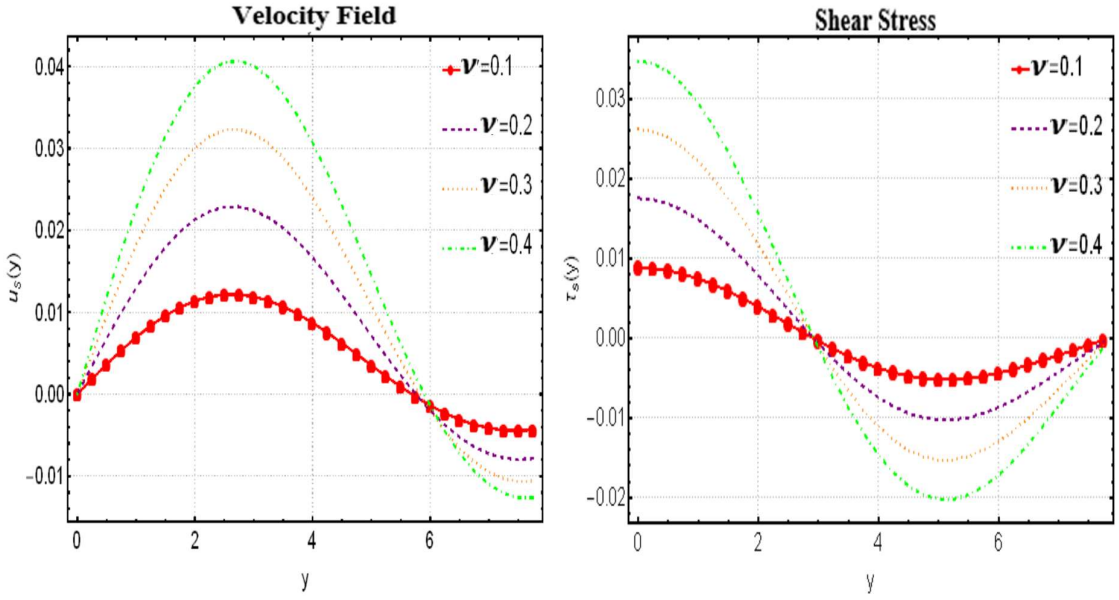

Fig.4.5. The velocity profile $u_s(y,t)$ and shear stress $\tau_s(y,t)$ for $U = 1$, $\lambda_1 = 2$, $\lambda_2 = 1$, $t = 2$, $\omega = 2$ and various ν.

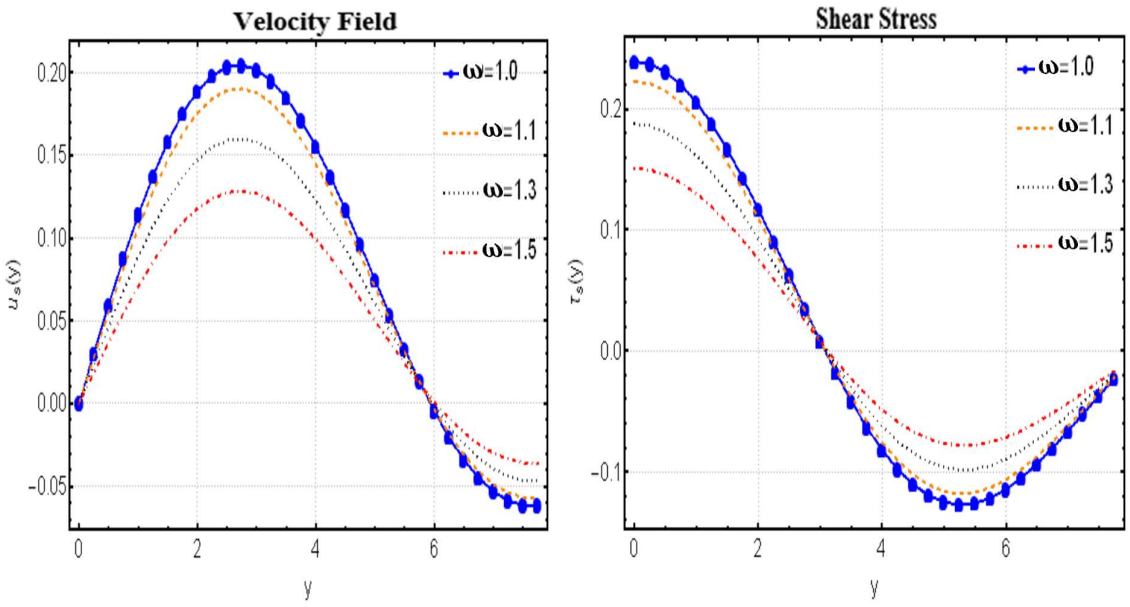

Fig. 4.6. The velocity field Profile $u_s(y,t)$ and shear stress $\tau_s(y,t)$ for $U = 1, t = 2, \lambda_1 = 2, \lambda_2 = 1, \nu = 0.63$ and various points of ω.

CHAPTER 5

CONCLUSION AND FUTURE WORK

5.1 Conclusion

We outline the key findings, discuss our contributions, and suggest directions for future research arising from this study. This research work aims to determine the exact solutions for sine and cosine boundary oscillations in a non-Newtonian fluid, as well as for the oscillating flow over a plate. In chapter three, the unsteady flows of an incompressible Maxwell fluid are analyzed, while chapter four extends this analysis to the Oldroyd-B fluid flowing over an oscillating plate. The Oldroyd-B model is a constitutive framework used to characterize viscoelastic fluids and can indeed predict phenomena related to relaxation and retardation times. Moreover, the velocity profile and corresponding shear stress for sine and cosine oscillations have been determined using integral transforms. These solutions conform to the specified initial and boundary conditions. The graphical results for the profile of velocity and associated shear stress over an oscillating plate, along with a comparison between Maxwell and Oldroyd-B fluids, highlight various interesting aspects of the results for different parameters. The general solutions are simplified and specified for the motion of a Newtonian fluid by eliminating the relaxation/retardation time parameter. This section summarizes the conclusions and suggestions derived from the study discussed in the preceding chapters.

We have provided exact solutions for sine and cosine oscillations over a plate of an incompressible upper convected Maxwell fluid in chapter 3. The infinite Fourier sine and Laplace transforms are employed to solve the governing equation and obtain the velocity and corresponding shear stress. The solution of the problem satisfies all initial and boundary conditions. For the boundary's sine and cosine oscillations, graphs have been made. The profiles of velocity and shear stress of the fluid are functions of increasing amplitude ω and

time t, respectively. The point of intersection in the fluid's motion for viscoelasticity is influenced by the relaxation time λ_1. Keep in mind that as the kinematic viscosity ν increases, both the fluid's velocity field and shear stress also increase. The fluid motion exhibits oscillatory effects with varying values of y .

In Chapter 4, we present the exact solutions for the Oldroyd-B fluid flowing across an oscillating plate that is incompressible and unstable. The purpose of this paper is to provide exact solutions for the velocity field and shear stress associated with the oscillating flows of an Oldroyd-B fluid over a flat plate. The motion is generated by the oscillation of the plate. These solutions can be expressed as both steady-state and transient components, obtained using the Fourier sine and Laplace transforms. The solution to the problem meets all initial and boundary conditions. It has been observed that the velocity field and shear stress of the fluid increase with time t and decrease with amplitude ω. The relaxation time λ_1 and the retardation time λ_2 influence the point of intersection in the fluid's motion for viscoelasticity. It should be noted that as the kinematic viscosity ν increases, both the velocity field of the fluid and the shear stress exhibit an increase. As the value of y varies, the effect on the fluid motion becomes oscillatory, showing changes in the fluid's behaviour depending on the position along y.

5.2 Future Work

In this thesis, we have presented a significant solution for the oscillation of plates with technical relevance to certain non-Newtonian fluids. Additionally, this study highlights the significant irregular characteristics of transient behavior in non-Newtonian fluids. Potential future developments and possible extensions to the existing energy equation involve exploring the effects of temperature on the Oldroyd-B parameters. However, analytical solutions for the velocity field and temperature profile of an Oldroyd-B fluid can also be derived when considering the influence of permeable media and physical forces, such as pressure gradients or external forces. We anticipate that this work will be valuable for analyzing more complex problems and will provide a foundation for various scientific and industrial applications.

REFERENCES

[1] M. Sheikholeslami., H. R. Kataria., and A. S. Mittal., "Effect of thermal diffusion and heat-generation on MHD nanofluid flow past an oscillating vertical plate through a porous medium." Journal of Molecular Liquids 257 (2018): 12-25.

[2] Patel, H. R., "Effects of heat generation, thermal radiation, and hall current on MHD Casson fluid flow past an oscillating plate in a porous medium." Multiphase Science and Technology 31, no. 1 (2019): 87-107.

[3] K. A. Abro., M. Hussain., and M. M. Baig., "A mathematical analysis of magnetohydrodynamic generalized burger fluid for the permeable oscillating plate." Punjab University Journal of Mathematics 50, no. 2 (2020): 97-111.

[4] R. Reyaz., Y. J. Lim., A. Q. Mohamad., M. Saqib., and S. Shafie., "Caputo fractional MHD Casson fluid flow over an oscillating plate with thermal radiation." Journal of Advanced Research in Fluid Mechanics and Thermal Sciences 85, no. 2 (2021): 145-158.

[5] M. F. Endalew., "Analytical study of heat and mass transfer effects on unsteady Casson fluid flow over an oscillating plate with thermal and solutal boundary conditions." Heat Transfer 50, no. 6 (2021): 6285-6299.

[6] A. Farooq., S. Rehman., A. N. Alharbi., M. Kamran., T. Botmart., and I. Khan., "Closed-form solution of oscillating Maxwell nano-fluid with heat and mass transfer," Scientific Reports 12, no. 1 (2022): 12-205.

[7] F. Asmat., W. A. Khan., M. Shamshuddin., S. O. Salawu., and M. Bouye., "Thermal analysis in an electrically conducting fluid with multiple slips and radiation along a plate: a case study of Stokes' second problem." Case Studies in Thermal Engineering 44 (2023): 102-831.

[8] S. Ghanami., and M. Farhadi, "Fluidic oscillators' applications, structures and mechanisms–a review." Challenges in Nano and Micro Scale Science and Technology 7, no. 1 (2019): 9-27.

[9] A. Guha., "Transport and deposition of particles in turbulent and laminar flow." *Annu. Rev. Fluid Mech.* 40, no. 1 (2008): 311-341.

[10] X. Zhang., R. Shah, S. Saleem., N. A. Shah., Z. A. Khan., and J. D. Chung., "Natural convection flow Maxwell fluids with generalized thermal transport and Newtonian heating." Case Studies in Thermal Engineering 27 (2021): 101-226.

[11] K. Hsiao., "Combined electrical MHD heat transfer thermal extrusion system using Maxwell fluid with radiative and viscous dissipation effects." Applied Thermal Engineering 112 (2017): 1281-1288.

[12] N. A. Asif., Z. Hammouch., M. B. Riaz., and H. Bulut., "Analytical solution of a Maxwell fluid with slip effects in view of the Caputo-Fabrizio derivative⋆." The European Physical Journal Plus 133 (2018):1-13.

[13] T. Hayat., M. I. Khan., M. Imtiaz., and A. Alsaedi., "Heat and mass transfer analysis in the stagnation region of Maxwell fluid with chemical reaction over a stretched surface." Journal of Thermal Science and Engineering Applications 10, no. 1 (2018): 1-6.

[14] M. B. Riaz., and N. Iftikhar, "A comparative study of heat transfer analysis of MHD Maxwell fluid in view of local and nonlocal differential operators." Chaos, Solitons & Fractals 132 (2020): 109-556.

[15] W. Yang., X. Chen., Z. Jiang., X. Zhang, and L. Zheng., "Effect of slip boundary condition on flow and heat transfer of a double fractional Maxwell fluid." Chinese Journal of Physics 68 (2020): 214-223.

[16] L. Liu., L. Feng., Q. Xu., L. Zheng, and F. Liu., "Flow and heat transfer of generalized Maxwell fluid over a moving plate with distributed order time fractional constitutive

models." International Communications in Heat and Mass Transfer 116 (2020): 104-679.

[17] T. Abdeljawad., M. B. Riaz., S. T. Saeed., and N. Iftikhar., "MHD Maxwell fluid with heat transfer analysis under ramp velocity and ramp temperature subject to non-integer differentiable operators." Computer Modeling in Engineering & Sciences 126, no. 2 (2021): 821-841.

[18] A. M. Megahed., "Improvement of heat transfer mechanism through a Maxwell fluid flow over a stretching sheet embedded in a porous medium and convectively heated." Mathematics and Computers in Simulation 187 (2021): 97-109.

[19] M. I. Asjad., R. Ali., A. Iqbal., T. Muhammad., and Y. Chu., "Application of water-based drilling clay-nanoparticles in heat transfer of fractional Maxwell fluid over an infinite flat surface," Scientific Reports 11, no. 1 (2021): 18-83.

[20] H. Hanif., "A computational approach for boundary layer flow and heat transfer of fractional Maxwell fluid." Mathematics and Computers in Simulation 191 (2022): 1-13.

[21] F. M. Abbasi., M. Mustafa., S. Shehzad., M. Alhuthali., and T. Hayat., "Analytical study of Cattaneo–Christov heat flux model for a boundary layer flow of Oldroyd-B fluid." Chinese physics B 25, no. 1 (2015): 14-70.

[22] A. Farooq., R. Ali., and A. C. Benim., "Soret and Dufour effects on three dimensional Oldroyd-B fluid." Physica A: Statistical Mechanics and its Applications 503 (2018): 345-354.

[23] A. Elhanafy., A. Guaily., and A. Elsaid., "Numerical simulation of Oldroyd-B fluid with application to hemodynamics." Advances in Mechanical Engineering 11, no. 5 (2019): 168-250.

[24] A. Hafeez., M. Khan, and J. Ahmed, "Flow of Oldroyd-B fluid over a rotating disk with Cattaneo–Christov theory for heat and mass fluxes." Computer methods and programs in biomedicine 191 (2020): 105-374.

[25] E. S.G. Shaqfeh., and B. Khomami., "The Oldroyd-B fluid in elastic instabilities, turbulence and particle suspensions." Journal of Non-Newtonian Fluid Mechanics 298 (2021): 104-672.

[26] M. Khan., A. Hafeez, and J. Ahmed, "Impacts of non-linear radiation and activation energy on the axisymmetric rotating flow of Oldroyd-B fluid." Physica A: Statistical Mechanics and Its Applications 580 (2021): 12-40.

[27] A. U. Awan., S. Riaz., K. A. Abro., A. Siddiqa., and Q. Ali., "The role of relaxation and retardation phenomenon of Oldroyd-B fluid flow through Stehfest's and Tzou's algorithms." Nonlinear Engineering 11, no. 1 (2022): 35-46.

[28] S. Bashir., M. Ramzan., H. A. S. Ghazwani., K. S. Nisar., C. A. Saleel., and A. Abdelrahman., "Magnetic dipole and thermophoretic particle deposition impact on bioconvective oldroyd-B fluid flow over a stretching surface with Cattaneo–Christov heat flux." Nanomaterials 12, no. 13 (2022): 21-81.

[29] S. Riaz., M. Sattar., K. A. Abro., and Q. Ali., "Thermo-dynamical investigation of constitutive equation for rate type fluid: a semi-analytical approach." International Journal of Modelling and Simulation 43, no. 3 (2023): 123-134.

[30] X. Wang., Fang, and Y. Wang., "A Finite Difference Method for Solving Unsteady Fractional Oldroyd-B Viscoelastic Flow Based on Caputo Derivative." Advances in Mathematical Physics 2023, no. 1 (2023): 89-90.

[31] R. M. Cotta., K. M. Lisboa., M. F. Curi., S. Balabani., J. Quaresma., J. S. Perez-Guerrero., E. N. Macêdo., and N. S. Amorim., "A review of hybrid integral transform solutions in fluid flow problems with heat or mass transfer and under Navier–Stokes equations formulation." Numerical Heat Transfer, Part B: Fundamentals 76, no. 2 (2019): 60-87.

[32] R. M. Cotta., K. M. Lisboa., and J. L. Z. Zotin., "Integral transforms for flow and transport in discrete and continuum models of fractured heterogeneous porous media." Advances in Water Resources 142 (2020): 103-621.

[33] H. Jafari., "A new general integral transform for solving integral equations." Journal of Advanced Research 32 (2021): 133-138.

[34] B. Mahfoud., and M. Moussaoui., "Buoyancy force and magnetic field effects on laminar vortex breakdown and fluid layers." Journal of Thermal Engineering 9, no. 1 (2023): 12-23.

[35] R. M. Cotta., M. Lachi., C. P. Naveira-Cotta., and A. E. Bruno., "Integral Transform Solution of Heat Conduction in Anisotropic Heterogeneous Media." Computational Thermal Sciences: An International Journal 16, no. 2 (2024): 50-75.

[36] S. Wang., P. Li., and M. Zhao., "Analytical study of the oscillatory flow of Maxwell fluid through a rectangular tube." Physics of Fluids 31, no. 6 (2019): 115-140.

[37] M. Jamil., A. Ahmed., and N. A. Khan., "Some exact traveling wave solutions of MHD Maxwell fluid in the porous medium." International Journal of Applied and Computational Mathematics 6 (2020): 1-18.

[38] S. Murtaza., M. Iftekhar, F. Ali., and I. Khan., "Exact analysis of the non-linear electro-osmotic flow of generalized maxwell nanofluid: applications in concrete-based nano-materials." IEEE Access 8 (2020): 96738-96747.

[39] C. Fetecau., R. Ellahi., and S. M. Sait., "Mathematical analysis of Maxwell fluid flow through a porous plate channel induced by a constantly accelerating or oscillating wall." Mathematics 9, no. 1 (2021): 40-90.

[40] E. S. Baranovskii., "Exact solutions for non-isothermal flows of second-grade fluid between parallel plates." Nanomaterials 13, no. 8 (2023): 1-40.

[41] Y. Cengel., and J. Cimbala., Ebook: Fluid mechanics fundamentals and applications (SI units). McGraw Hill, 2013: 180-250.

[42] K. A. Abro., and A. A. Shaikh., "Exact analytical solutions for Maxwell fluid over an oscillating plane." Sci. Int. (Lahore) ISSN 27 (2020): 923-929.